Theme B: Planning and inspection

Theme B

Planning and Inspection

Leere Seite
Blank page
Page vide

Probability-Based Optimisation of Inspection Intervals for Steel Bridges

Christian CREMONA
Dr. Eng.
LCPC
Paris, France

Christian Crémona graduated from the École Nationale des Travaux Publics de l'État (F) and obtained his PhD degree from the University of Wales (UK). Since 1992, he has been involved in research into traffic and wind load effects on bridges and bridge reliability assessment.

Summary

The fatigue safety of steel bridges is achieved through design of individual components and inspections with subsequent repair of detected cracks. Each safety item has a certain cost and it is of importance to minimise the total expected cost for the lifetime of the component. The optimisation parameters are the inspection times, but other variables (material properties, inspection qualities,...) can be also introduced. Two optimisation problems are treated in this paper. The first one concerns the optimisation of the next inspection time, while the second one treats of the optimisation of the regular inspection interval during the component lifetime. An example of a welded joint highlights the different concepts. It has to be noticed that the techniques presented in the paper are not restricted to fatigue problems, but can be applied to a wide variety of deterioration phenomena.

1. Introduction

Maintenance and rehabilitation of existing structures has become of great concern for public or private owners during the last decades. All the structures made by men are time-degrading because of phenomena such as corrosion, fatigue, erosion,... induced sometimes by poor durability design, lack of quality control or absence of regular inspection and maintenance actions.

Budgets for maintenance and rehabilitation are always limited. In order to rationalise maintenance actions, management systems have been developed, helping to a standardisation of the procedures through the development of inspection manuals and the implementation of databases. Experience acquired with these procedures leads today to define other approaches in which rationality is based on the optimisation of maintenance costs. This optimisation requires methods which take into account technical, economical, management points of view as well as theoretical or practical aspects. Offshore engineering has already successfully rationalised its maintenance actions (see for instance [1], [2]) by using probabilistic concepts. The present paper attempts to illustrate such an approach in the field of steel bridges with respect to the problem of welded joints damaged by fatigue. In welded joints, the cracks are often localised at the weld. The welds induce some defects which help small cracks to appear. They are growing under loading and can lead to the joint failure. The conditions governing crack growth propagation are

numerous, and in general, random. Therefore, an appropriate analysis of fatigue phenomena consists by treating the problem in a probabilistic manner. But, the probabilistic model must be flexible enough to include inspection results with their qualities for assessing damage in a better manner. Such an approach must help to consider all the events (inspections, repairs, failure) which can occur during the conventional lifetime of the joint. As costs can be linked to these events, it is then possible to build an optimisation procedure aiming to minimise the total maintenance cost with respect to conventional reliability degrees.

2. Models

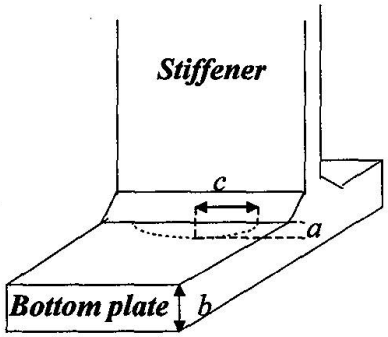

Fig.1 Crack details in a welded joint

Two types of model are used to determine a management strategy: event models and maintenance models. The event models are mathematical models which describe events occurring in the component. For welded joints, these models contain the fatigue crack growth model and the detection model. These mathematical models permit to assess the corresponding probabilities of events occurrence. The maintenance models are linked to the strategy of maintenance and management. In these models, the events probabilities determined with the event models are combined with costs for providing total expected maintenance costs.

2.1. Crack growth model

The model used in this paper is the Paris law corresponding to the opening of a semi-elliptical crack in the bottom plate of a « stiffener-bottom plate » welded joint (Figure 1)

$$\frac{da}{dN} = C(\Delta K)^m = C\left[Y(a,c)M_k(a)\Delta S\sqrt{\pi a}\right]^m \tag{1}$$

where

- a is the crack size, c half the crack length, b the bottom plate thickness,
- N is the number of cycles, ΔK the stress intensity factor range, ΔS the stress range,
- $Y(a, c)$ is the stress intensity geometry correction factor, $M_k(a)$ the stress intensity concentration correction factor, C and m two material parameters.

Under the threshold stress intensity range ΔK_{th}, the crack does not grow. Equation (1) does not distinguish damaging and non damaging cycles. The modified model of reference [3] introduces a correction function $G(a, c)$ which allows this discrimination:

$$\frac{da}{dN} = C\left(Y(a,c)M_k(a)\sqrt{\pi a}\right)^m G(a,c)\left(\frac{2E(\Delta S)}{\sqrt{\pi}}\right)^m \Gamma\left(1+\frac{m}{2}\right) \tag{2}$$

where

$$G(a,c) = 1 - \frac{1}{\Gamma\left(1+\frac{m}{2}\right)}\gamma\left(1+\frac{m}{2};\frac{1}{2}\frac{(\Delta K_{th})^2}{\left(\sqrt{\frac{2}{\pi}}\mathrm{E}(\Delta S)Y(a,c)M_k(a)\sqrt{\pi a}\right)^2}\right) \tag{3}$$

$E(\Delta S)$ is the mean of the stress range process. $\Gamma(.)$ and $\gamma(.,.)$ are respectively the complete and incomplete Gamma functions. $N(t) = \nu_0 t$ is the number of cycles at time t. Equations (2) and (3) have been obtained under the assumption that the stress ranges follows Rayleigh distributions and by using the equivalent stress range approach [4].

A safety margin expresses the frontier between damage and non damage. A straightforward safety margin for fatigue reliability assessment can be defined by $Z(t) = a(t) - a_c$, where a_c is the critical crack size, which can be chosen to a conventional value or according to a fracture criterion. $a(t)$ is the crack size at time t after $N(t)$ cycles. The integration of Equation (2) between an initial crack size a_0 and a_c is equivalent to another safety margin :

$$M(t) = \int_{a_0}^{a_c} \frac{dx}{\left(Y(a,c)M_k(a)\sqrt{\pi a}\right)^m G(a,c)} - CN(t)\left(\frac{2E(\Delta S)}{\sqrt{\pi}}\right)^m \Gamma\left(1+\frac{m}{2}\right) \tag{4}$$

2.2. Detection model

A measurement system cannot detect a crack when it is too small. A threshold value exists and corresponds to the detection level under which detection is no longer reliable. This threshold crack size, a_d is the smallest detectable crack size allowable by the measurement system. The probability to detect a crack depends on a_d, and on the precision of the system. In general, a_d is never precisely known, and therefore, has to be considered as a random variable. The detection probability is consequently the probability that the crack size is greater than a_d. If x is the crack size and $F(.)$ the distribution function for a_d, the probability to detect a crack is then:

$$P_d(x) = P(x \geq a_d) = F(x) \tag{5}$$

The knowledge of $P_d(x)$ is therefore sufficient for determining the distribution function of a_d. Several models have been developed for explaining the uncertainties met by using Non Destructive Inspection techniques [4]. For instance, the ultrasonic detection method leads to a detection level a_d which can be modelled by a lognormal distribution.

2.3 Events margins

Qualitative or quantitative information can be given by inspections. Each of these results is an event, associated to an event margin H and to an occurrence probability.

Qualitative inspection results are information upon the detection or the non detection of an event related to a particular phenomenon. The information is expressed by:

$$H \leq 0 \tag{6}$$

For fatigue crack growth propagation, the non-detection of a crack size A_i after N_i cycles corresponds to an event where the crack size $a(N_i)$ is *smaller than* A_i. The no detection event is expressed by

$$H_{nd}(a_i) = -\int_{a_0}^{A_i} \frac{dx}{\left(Y(a,c)M_k(a)\sqrt{\pi a}\right)^m G(a,c)} + CN_i\left(\frac{2E(\Delta S)}{\sqrt{\pi}}\right)^m \Gamma\left(1+\frac{m}{2}\right) \leq 0 \tag{7}$$

The detection event is the complementary of the previous one and the event is then:

$$H_d = \int_{a_0}^{A_i} \frac{dx}{\left(Y(a,c)M_k(a)\sqrt{\pi a}\right)^m G(a,c)} - CN_i\left(\frac{2E(\Delta S)}{\sqrt{\pi}}\right)^m \Gamma\left(1+\frac{m}{2}\right) \leq 0 \tag{8}$$

Quantitative inspection results correspond to measurements of an event related to a particular phenomenon. The information is expressed by:

$$H = 0 \tag{9}$$

For fatigue crack growth propagation, the detection with measurement corresponds to an event where the crack $a(N_i)$ after N_i cycles, is *equal* to A_i, measurement at time t_i. The « detection with measurement » event is expressed by

$$H = \int_{a_0}^{A_i} \frac{dx}{\left(Y(a,c)M_k(a)\sqrt{\pi a}\right)^m G(a,c)} - CN_i\left(\frac{2\mathrm{E}(\Delta S)}{\sqrt{\pi}}\right)^m \Gamma\left(1+\frac{m}{2}\right) = 0 \tag{10}$$

2.4 Maintenance model

The maintenance model which has been used, is the conditional maintenance with regular inspection interval. A conditional maintenance requires to define criteria or conditions according to which maintenance actions will be engaged. This has to be made by quantifying crack sizes by a detection method and by ranging crack sizes in a finite number of severity classes.

Let us assume that this finite number of classes is limited to (n_R+1) where the first class corresponds to non detectable cracks. Let us call this class $I_0 = [0, a_d[$ where a_d corresponds to the smallest crack size which can be detected. If there are n_R types of possible repairs, then it follows that any crack with size $a \in I_i = [a_{i-1}, a_i[$ is repaired by the repair technique N.*i*. Let us note that the decision interval $I_1 = [a_d, a_1[$ can correspond to a detection followed by no repair actions. Figure 2 illustrates the different scenarios occurring at each inspection time according to a conditional maintenance strategy. T_s is a reference period which can be the next inspection time or the conventional lifetime T_f. The inspection events are therefore defined as it follows:

- the event corresponding to a non detection is $\left\{H^0 \le 0\right\}$,
- the event corresponding to a repair method N.*i* is $\left\{H^i \le 0\right\}$.

In fact, the events have to be rigorously written:

- $\left\{H^0 \le 0\right\} = \left\{H_{nd}(a_d) \le 0\right\}$,
- $\left\{H^1 \le 0\right\} = \left\{H_d(a_d) \le 0 \cap H_{nd}(a_1) \le 0\right\}$
- $\left\{H^i \le 0\right\} = \left\{H_d(a_{i-1}) \le 0 \cap H_{nd}(a_i) \le 0\right\}$ for $i = 2, \cdots, n_R - 1$
- $\left\{H^{n_R} \le 0\right\} = \left\{H_d(a_{n_R-1}) \le 0\right\}$.

Nevertheless, for the sake of simplicity, the first notation will be kept in the following developments. Each action at each inspection has an effect on the event and safety margins at the next inspection time. It is therefore necessary to introduce another notation for describing the events sequences. For instance, with an action k at time t_1 and an action l at time t_2, the safety margin at time $t_2 \le t \le t_3$ will be denoted $M^{k,l}$ and the event margin at time t_2 will be denoted $H^{k,l}$. $M(t)$ will still define the safety margin before the first inspection time.

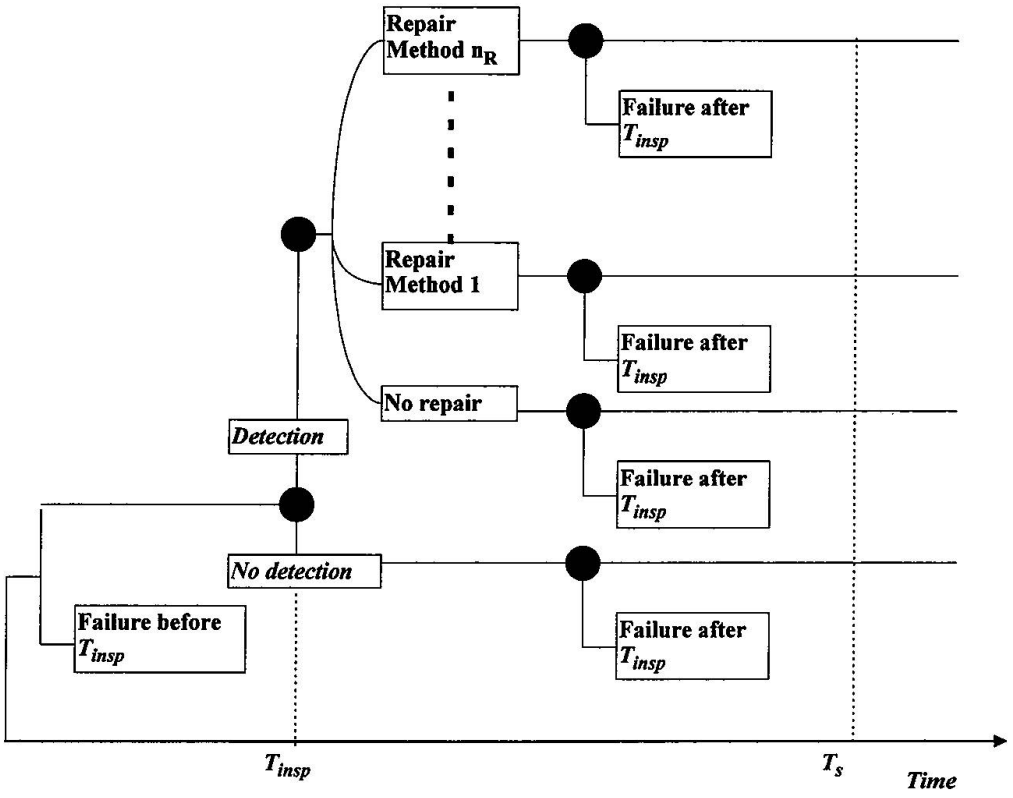

Fig.2 Events tree for a conditional maintenance model

3. Probabilities of failure and repair

Let us note $P_f(t)$ the probability of failure at time t. The reliability index β is defined by (First Order Reliability approach):

$$\beta(t) = -\Phi^{-1}\left(P_f(t)\right) \tag{11}$$

If we note $\Delta P_f(t_i, t)$ the probability of failure in the time interval $]t_i, t]$, then it follows:

– for $0 \le t \le t_1$:

$$P_f(t) = \hat{P}_f(t) = P(M(t) \le 0) \tag{12}$$

– for $t_1 \le t \le t_2$:

$$\begin{aligned} P_f(t) &= P_f(t_1) + \Delta P_f(t_1, t) \\ &= P_f(t_1) + \Delta P_f^0(t_1, t) + \cdots + \Delta P_f^{n_R}(t_1, t) \\ &= P_f(t_1) \\ &\quad + P\left(M(t_1) > 0 \cap H^0 \le 0 \cap M^0(t) \le 0\right) \\ &\quad \vdots \\ &\quad + P\left(M(t_1) > 0 \cap H^{n_R} \le 0 \cap M^{n_R}(t) \le 0\right) \end{aligned} \tag{13}$$

and so on for each inspection time. The probability of repair N.r ($r \geq 2$) is determined by

$$P_{rep}(t_1) = P\left(M(t_1) > 0 \cap H_r \leq 0\right) \tag{14i}$$

$$\begin{aligned} P_{rep}(t_2) &= P_{rep}^{0,r}(t_2) + \cdots + P_{rep}^{n_R,r}(t_2) \\ &= P\left(M(t_1) > 0 \cap H^0 \leq 0 \cap M^0(t_2) \cap H^{0,r} \leq 0\right) \\ &\vdots \\ &+ P\left(M(t_1) > 0 \cap H^{n_R} \leq 0 \cap M^0(t_2) \cap H^{n_R,r} \leq 0\right) \end{aligned} \tag{14ii}$$

and so on, for each inspection time.

4. Optimisation of the next inspection time

The problem consists in the determination of an optimal inspection time t_1 which minimises the total expected cost. The inspection time t_1 must fulfil the condition $t_1 \leq T_s$, where T_s corresponds to the time with a reliability equal to the minimum reliability $\beta_{\min}$ which can be accepted. The expected cost models are therefore the following:

- Expected inspection cost:

$$C_I(t_1) = C_{ins}\left(1 - P_f(t_1)\right)\frac{1}{(1+\alpha)^{t_1}} \tag{15}$$

- Expected repair cost:

$$C_R(t_1) = \sum_{r=2}^{n_R} C_{rep}(r) P_{rep}^r(t_1)\frac{1}{(1+\alpha)^{t_1}} \tag{16}$$

- Expected failure costs:

$$C_F(t_1) = C_f\left(P_f(t_1) - P_f(t_0)\right)\frac{1}{(1+\alpha)^{t_1}} \tag{17i}$$

$$C_F(T_s) = C_f\left(P_f(T_s) - P_f(t_1)\right)\frac{1}{(1+\alpha)^{T_s}} \tag{17ii}$$

where C_{ins}, $C_{rep}(r)$, C_f are the expected inspection cost, the expected repair cost and the expected failure cost respectively, and α is the rate of interest.

The inspection time t_1 is therefore determined as the optimal solution of the minimisation problem

$$\min_{t_1} C_T(t_1) = \min_{t_1}\left(C_I(t_1) + C_R(t_1) + C_F(t_1) + C_F(T_s)\right) \tag{18}$$

The time t_0 can be any time after the putting in service of the welded joint. The time t in the models has nevertheless to be adjusted in order to take into account of this delay.

5. Optimisation of the next inspection time with observation

Inspections provide useful information for updating component reliability. In that case, the probabilities of repair and failure have to be modified by using a bayesian approach which replaces all the probabilities by conditional probabilities. If qualitative and quantitative inspection results are available, then the updated probability of failure can be expressed by :

- for $0 \le t \le t_1$:

$$P_f^{up}(t) = P\left(M(t) \le 0 / \bigcap_{i=1}^{p} \left(\tilde{H}_i^1 \le 0 \right) \cap \bigcap_{i=1}^{q} \left(\tilde{H}_i^2 = 0 \right) \right) \tag{19i}$$

where :

$\left(\tilde{H}_i^1\right)_{1 \le i \le p}$ and $\left(\tilde{H}_i^2\right)_{1 \le i \le q}$ are the qualitative and quantitative inspection results respectively.

- for $t_1 \le t \le t_2$:

$$\begin{aligned} P_f^{up}(t) &= P_f^{up}(t_1) + \Delta P_f^{up}(t_1, t) \\ &= P_f^{up}(t_1) + \Delta P_f^{up,0}(t_1, t) + \cdots + \Delta P_f^{up,n_R}(t_1, t) \\ &= P_f^{up}(t_1) \\ &+ P\left(M(t_1) > 0 \cap H^0 \le 0 \cap M^0(t) \le 0 / \bigcap_{i=1}^{p} \left(\tilde{H}_i^1 \le 0 \right) \cap \bigcap_{i=1}^{p} \left(\tilde{H}_i^2 = 0 \right) \right) \\ &\vdots \\ &+ P\left(M(t_1) > 0 \cap H^{n_R} \le 0 \cap M^{n_R}(t) \le 0 / \bigcap_{i=1}^{p} \left(\tilde{H}_i^1 \le 0 \right) \cap \bigcap_{i=1}^{p} \left(\tilde{H}_i^2 = 0 \right) \right) \end{aligned} \tag{19ii}$$

6. Optimisation problem

Here, the problem consists in the determination of an inspection interval Δt which induces a minimal maintenance expected cost during the conventional lifetime T of the component. For this purpose, the number of inspections n is first given, and then the total expected cost is evaluated. The procedure is performed for different number of inspections and the different expected costs are compared; the value n which provides the smallest cost gives to the optimal inspection period. Let us precise that some constraints have to be also fulfilled, as the optimisation problem beneath illustrates :

$$\min_{\Delta t} C_T(\Delta t) = \min_{\Delta t} \left[\sum_{i=1}^{n} \left[C_I(\Delta t) + C_R(\Delta t) + C_F(\Delta t) \right] + C_F\left(T_f t\right) \right] \tag{20i}$$

under constraints

$$\beta\left(T_f\right) \ge \beta_{\min};\ \Delta t_{\min} \le \Delta t \le \Delta t_{\max};\ \ 0 \le T_f - n\Delta t \le \Delta t_{\max} \tag{20ii}$$

Δt_{min}, Δt_{max} are minimal and maximal time intervals for inspections.

7. Example of a welded joint

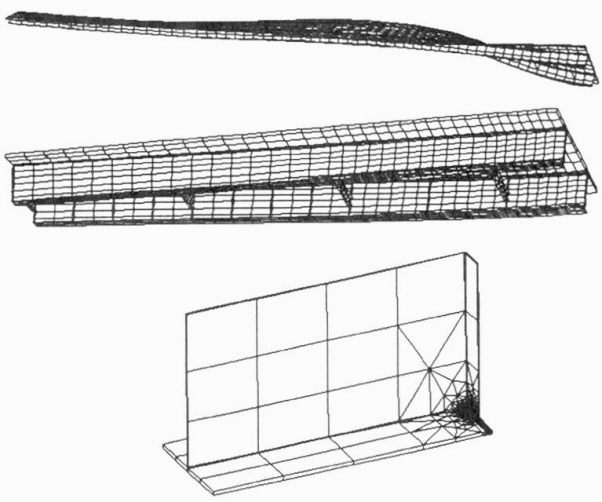

Fig 3 *Finite elements modelling of the joint*

A particular welded joint « bottom plate/stiffener » from a typical steel bridge has been here considered (Figure 1 and Figure 3). It is subject to 1.7 millions of stress variation cycles per year, with 11.0 MPa for mean. These values result from computations using the influence surfaces of the bridge and recorded heavy traffic data. The critical crack size is taken equal to the thickness of the bottom plate (crossing crack). The stress intensity geometry correction factor $Y(a, c)$ is the solution of Newman and Raju [5]. $Y(a, c)$ introduces the crack shape ratio a/c. This ratio is function of different parameters (local geometry, crack size a, stress intensity variation,...) which are difficult to model because of lack of information. For this reason, it is more suitable to use statistical distributions for describing the crack shape ratio according to the type of joint. For transversal welded joints, Yamada and al. [6] propose to choose lognormal distributions.

$$Y(a,c) = \frac{1}{\sqrt{1+1.464\left(\frac{a}{c}\right)^{1.65}}}\left[Y_1(a,c) + Y_2(a,c)\left(\frac{a}{b}\right)^2 + Y_3(a,c)\left(\frac{a}{b}\right)^4\right]$$

$$Y_1(a,c) = 1.13 - 0.09\frac{a}{c};\quad Y_2(a,c) = \frac{0.89}{0.2+\frac{a}{c}} - 0.54 \tag{21}$$

$$Y_3(a,c) = 0.5 - \frac{1}{0.65+\frac{a}{c}} + 14\left(1-\frac{a}{c}\right)^{24}$$

The stress intensity concentration factor $M_k(a,b)$ is given by an exponential model:

$$M_k(a) = v\left(\frac{a}{b}\right)^w \tag{22}$$

According to table 1 which provides the statistical properties of the different model variables, it is possible to evaluate the evolution of the reliability index related to the probability of failure as a function of the time t (Figure 4) given by :

$$\hat{P}_f = P(M(t) \le 0) \tag{23}$$

Variable	Type	Mean	C.O.V.	Unit
a_0	Ln.	*0.0006*	*5%*	*m*
$a_c = b$	D.	*0.0175*	/	*m*
a_{rep}	Ln	*0.001*	*10%*	*m*
a_2	D	*0.003*	/	*m*
a_d	Ln.	*0.002*	*10%*	*m*
m	N.	*2.85*	*5%*	*adim*
C	Ln.	8.10^{-12}	*10%*	*adim*
v	Ln.	*0.77*	*2%*	*adim*
w	N.	*-0.24*	*6%*	*adim*
a / c	Ln.	*0.39*	*4%*	*adim*
v_0	D	*1700000*	/	*cycles/year*
ΔK_{th}	D	*0*	/	*MPa*
$E(\Delta S)$	D.	*11.0*	/	*MPa*
b	D.	*0.035*	/	*m*

Table 1 *Statistical characteristics*
$(\rho(\ln C, m) = -0.9$ *and* $\rho(\ln v, w) = 0.99)$

Repair cost)	*4.2%*
Inspection cost	*0.2%*
Failure cost	*100%*
Conventional lifetime T_f	*100 years*
Rating of interest α	*4%*
Δt_{min}	*5 years*
Δt_{max}	*20 years*
β_{min}	*3.5*

Table2 *Optimisation characteristics*

The minimum reliability index β_{min} is obtained for the time $t \approx 22$ *years*. This time will be used as the reference period T_s for the determination of the next inspection time.

The optimisation problem introduced in Section 4 is used for determining the first inspection time. No information is available, and the costs are all expressed in terms of percentages of the cost of failure [7]. The different expected costs can be calculated versus the next inspection time $t_1 \leq T_s = 22$ *years*.

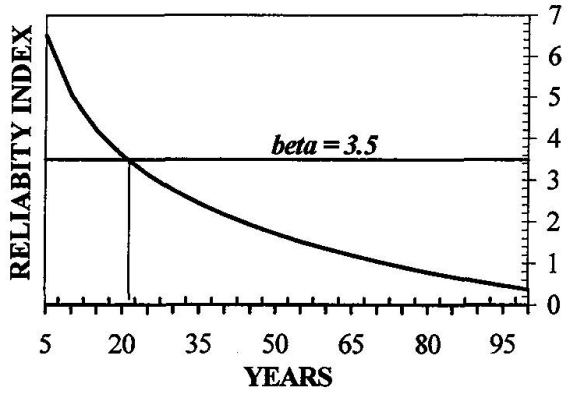

Fig.4 *Welded joint time-varying reliability*

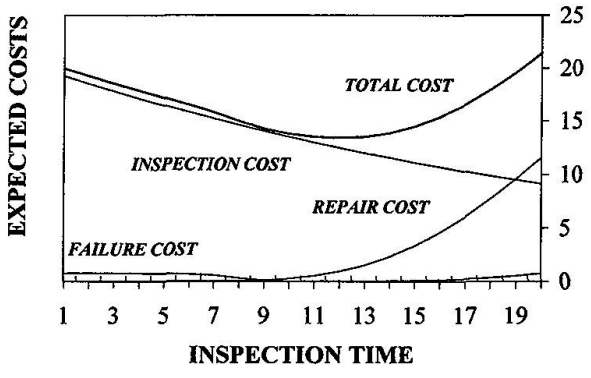

Fig.5 *Expected cost variation as a function of next inspection time*

Figure 5 illustrates the evolution of these costs according to the data of Table 2. The conditional maintenance strategy has three issues: no detection, detection with no repair and detection with repair by welding. The corresponding action intervals I_i are respectively $[0, a_d[$, $[a_d, a_2 = 3\ mm[$ and $[a_2, b[$. The computations of the probabilities of failure and repair are obtained through optimised recursive schemes requiring multidimensional integrals for the calculus of the probabilities in event series systems [7]. For this welded joint, the minimum total expected cost is obtained for an inspection time $t_1 = 12$ *years*. The reliability index $\beta(20) = -\Phi^{-1}(P_f(20))$ is *4.6*.

Figure 5 shows that the expected repair cost is non zero; consequently, a repair has to be expected at $t = 12$ *years*.

The optimal inspection interval is given by the optimisation problem of section 6. To solve this problem is very time consuming, and a lot of work has to be done for improving it. The optimal inspection interval is of *10 years*. The final reliability index is *4.0*.

8. Conclusions

The paper has presented a methodology for optimising the inspection programme for components in steel bridges. The concepts have been applied to welded joints with respect to fatigue failure and an example is given for highlighting the different theoretical aspects. The optimised inspection intervals are regular intervals, but the approach of Section 6 can be generalised to variable inspection intervals [7], but the corresponding computations are time consuming. It has to be noticed that the individual inspection intervals have to be combined, in a final stage, for providing a final inspection interval at the structure level. This can be performed by using qualitative combinations (expensive actions regrouping, available budget,...) as well as quantitative combinations of the individual inspection intervals [8]. Some additional effort is nevertheless still needed in order to assess the sensitivity of the results to change in the parameters involved in the cost optimisation procedure.

References

1. MADSEN H.O., SORENSEN J.D., OLESEN R., Optimal Inspections Planning for Fatigue Damage of Offshore Structures, Proceedings ICOSSAR 89, San Francisco, USA, 1989, pp.2099-2106.
2. GOYET J., MAROINI A., Offshore Platform Reliability. Optimal Inspection and Repair Planning: an Application with a Sensitivity Study using IMREL Methodology, International Conference on Fatigue of Welded Components and Structures, Senlis, France, 1996, pp.149-162.
3. CREMONA C., Applications de la Théorie de la Fiabilité à la Sécurité d'Eléments Structuraux d'Ouvrages d'Art, Collection Etudes et Recherches, N.17, LCPC, Paris, France, 1995.
4. CREMONA C., Reliability Updating of Welded Joints Damaged by Fatigue, International Journal of Fatigue, to be published in 1996.
5. BS PD 6493: 1991, Guidance on Methods for Assessing the Ability of Flaws in Welded Structures, British Standards Institution, London, 1991.
6. YAMADA Y., NAGOATSU S., MITSUGI Y., Evaluation of Scatter of Fatigue Life of Welded Details using Fracture Mechanics", Department of Civil Engineering, Nagoya University, 1989.
7. SEMPERE H., Maintenance de la Fiabilité des Ponts Routiers: Optimisation des Plannings d'Inspection et de Réparation, Mémoire de Fin d'Etudes, Université Blaise Pascal, Clermont-Ferrand, 1996.
8. CREMONA C., Optimisation de la Fiabilité et de la Maintenance des Ouvrages d'Art Métalliques, Revue Française de Mécanique, to be published in 1997.

System Reliability for Condition Evaluation of Bridges

Allen C. ESTES
Graduate Student
Univ. of Colorado
Boulder, CO, USA

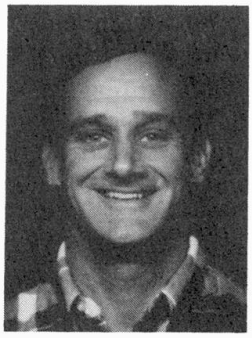

Allen C. Estes is a Lieutenant Colonel in the U.S. Army Corps of Engineers and is working toward his Ph.D. in Structural Engineering at the University of Colorado.

Dan M. FRANGOPOL
Professor
Univ. of Colorado
Boulder, CO, USA

Dan M. Frangopol is Professor of Civil Engineering at the University of Colorado. He received his civil engineering degrees from the Institute of Civil Engineering, Bucharest, Romania (1969) and the University of Liege, Belgium (1976). His research activities include reliability analysis and design of buildings and bridges, bridge management systems, and structural optimization.

Summary

For many bridges which were designed and built before structural reliability methods were applied to structural design, there is an urgent need to quantify their safety from a system reliability viewpoint. Optimum inspection, repair, and replacement strategies need to be developed based on minimizing the expected cost of keeping the system reliability above the established target level during the anticipated remaining service life of these bridges. These strategies need to be updated over time through timely inspections based on changing conditions. This study proposes a methodology for a system reliability-based condition evaluation of existing highway bridges. The approach is illustrated for an existing steel bridge located in Colorado. The initial optimum repair strategy is updated using both biennial visual inspections and specific non-destructive evaluation testing.

1. Introduction

Over the past several decades, the concepts and methods of structural reliability have developed rapidly and become widely accepted among researchers and increasingly acknowledged among practicing engineers. The United States has a national inventory of almost 600,000 highway bridges, many of which have deteriorated substantially and will require large expenditures to repair. A system reliability approach to optimizing the inspection and repair of these bridges will provide a more efficient use of the scarce funding resources by providing an acceptable level of safety at a minimum expected cost. For many bridges which were designed and built before structural reliability methods were applied to structural design, there is an urgent need to quantify their safety from a system reliability perspective.

This study proposes a methodology for condition evaluation of existing highway bridges based on system reliability. The technique is illustrated using State Highway Bridge E-17-AH, located in the metro Denver area of Colorado. An optimum lifetime repair strategy is developed for the bridge by minimizing the expected lifetime cost and maintaining a prescribed level of system safety throughout the life of the bridge. This repair strategy is only as valid as the assumptions that were made when the bridge was placed in service. The repair strategy must be updated and revised throughout the life of the bridge based on the results of periodic inspections. The methodology for revising the repair strategy for Bridge E-17-AH is developed based on both the mandatory biennial visual inspections and some specific non-destructive evaluation (NDE) testing.

2. System reliability approach to the repair optimization of an existing highway bridge

A time-dependent system reliability approach is applied to optimize the repair strategy for an existing highway bridge (Colorado State Highway Bridge E-17-AH). The bridge is on State Highway 33 in Denver, Colorado, and has three 13.36 m simply-supported steel-concrete composite spans. The 12.18 m wide roadway carries four lanes of traffic with an Average Daily Traffic (ADT) of 8500 vehicles. The deck is reinforced concrete and the steel girders are standard rolled shapes with simple-span supports. The interior span supports are reinforced concrete pier columns with a pier cap, four supporting square tapered columns, and individual column footings. The concrete abutments are supported by concrete piles cased in steel. A local railroad spur runs underneath the bridge. The cross section of the superstructure is shown in Fig.1(a) where the girders are classified as exterior (E), interior-exterior (I-E), and interior (I).

Using 24 separate random variables, the intact bridge was analyzed with respect to 16 different failure modes including moment failure of the slab, moment and shear failure of the girders, and multiple failure modes of the pier cap, columns and footings. Limit state equations were developed and the reliability of each component was computed separately. The bridge system was modeled as a series-parallel model. Both the component reliabilities and the system reliability of the bridge were computed. A simplified system model for the bridge where it is assumed that the superstructure will not fail until three adjacent girders have failed is shown in Fig. 1(b). The simplifying assumptions, a more refined model, and a complete description of these calculations are given in Estes [5].

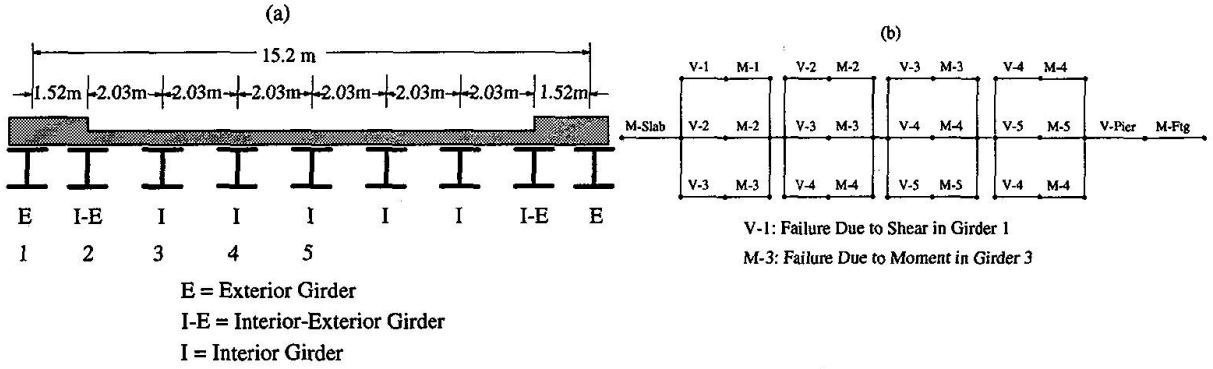

Fig. 1 Colorado State Highway Bridge E-17-AH: (a) Designation of girders, and (b) Simplified series-parallel model

The reliability of the bridge system is decreasing over time as the live load increases and the structure deteriorates. The time-dependent live-load shear and moment effects are a function of the length of the span, the average daily truck traffic, and the shear and moment caused by an AASHTO HS-20 truck as proposed by Nowak [9]. It is assumed that the slab and pier cap deteriorate due to the penetration of chlorides through the concrete as suggested by Thoft-Christensen [11]. Corrosion begins once the chlorides reach a critical threshold concentration at the level of the reinforcing steel. The time required for corrosion to begin is the corrosion initiation time T_I. The rate of corrosion r_{corr} determines the amount of section loss in the reinforcing steel over time. The girders are corroding using the model developed by Albrecht and Naeemi [1]. The corresponding section loss reduces the web area and plastic section modulus over time. This reduces the girder shear and moment capacities, respectively. The deterioration process introduces new random variables into the limit state equations which include diffusion rates, chloride surface concentration, and corrosion parameters.

A minimum allowable (i.e., target) lifetime system reliability index $\beta_{T,system\ life} = 2.0$ is established. The bridge is inspected every two years and anytime the system reliability of the bridge falls below the prescribed minimum, some type of repair or replacement must be made. After considering the initial cost of the bridge, Colorado Department of Transportation (CDOT) cost documents [3] and conversations with experts at CDOT, the following repair options and their associated present day (1996) costs were established: (a) Option 0: Do nothing → \$0; (b) Option 1: Replace deck → \$225,600; (c) Option 2: Replace exterior two girders (E and I-E in Fig. 1(a)) → \$229,200; (d) Option 3: Replace exterior two girders and entire deck → \$341,800;

(e) Option 4: Replace entire superstructure → $487,100; and (f) Option 5: Replace entire bridge → *$659,900.*

For option 1 (replace deck), Fig.2 shows the time-dependent reliabilities of the bridge system and of all components shown in Fig. 1(b). The deck is replaced when $\beta_{system} \leq 2.0$. Consequently, the deck is replaced twice at years 50 and 94 of the bridge life. At year 106, a deck replacement is not sufficient to improve β_{system} to a value larger than 2.0. Due to the parallel nature of the system, the reliability of some components are allowed to fall below $\beta_{T,system\ life}$ =2.0. Due to varying deterioration rates, the critical component early in the life of the structure is not necessarily the most important later on.

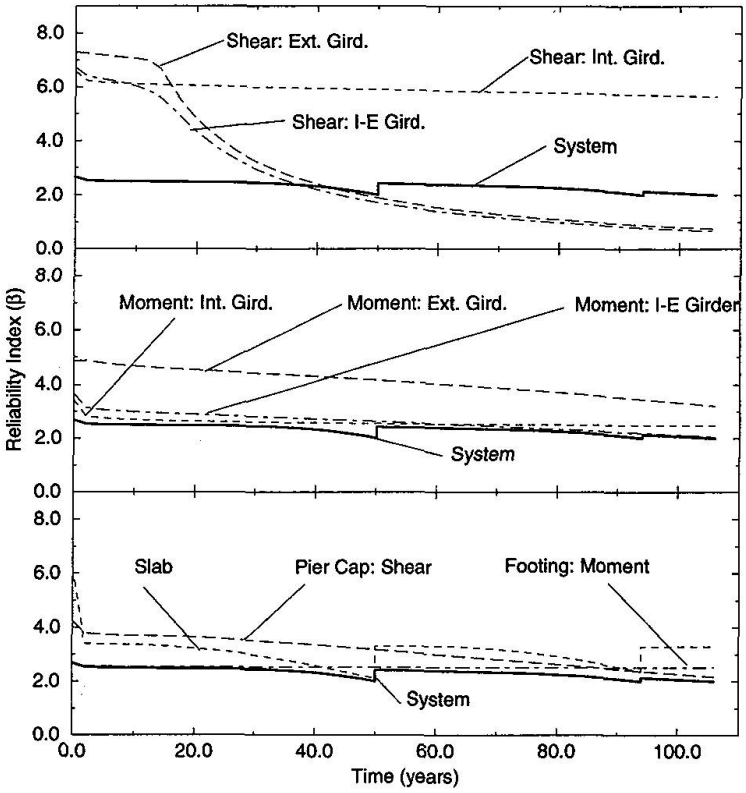

***Fig. 2** Results of repair option 1: Replace deck on Bridge E-17-AH using series-parallel system model requiring the failure of three adjacent girders*

Let's assume the bridge is placed in service in 1996. Accounting for all combinations of options and using an assumed discount rate of 2%, the possible repair strategies and their associated present value costs are shown in Fig. 3. The analysis continued until replacement of the bridge (i.e., option 5) becomes the only available solution. From Fig. 3, the optimum strategy can be determined for the expected life of the bridge. For example, for a life of 50 years, no action should be taken; for 50-94 years, replace the deck at year 50 ($83,813); 94-106 years, replace the deck at year 50 and year 94 ($118,881); 106-108 years, replace the slab at year 50 then replace the exterior two girders and slab at year 94 ($136,945); and after 108 years, replace the slab at year 50 then replace the bridge at year 94 ($186,393).

The bridge was analyzed for several different series-parallel system models where the failure of two adjacent girders or failure of a single girder would cause failure of the superstructure. Other parameters such as random variable correlation, deterioration rates, and discount rates were varied and often produced very different results. A repair strategy based on uncertain information must be updated throughout a structure's life based on inspection results. Without a series of specialized tests, the reliability of the bridge when placed in service is based on the same information available to the designer. During the design phase of a structure, the random variables are based on data from other projects, manufacturer specifications, and available literature. For an existing structure, the availability of material tests and field measurements can improve the knowledge of random variables.

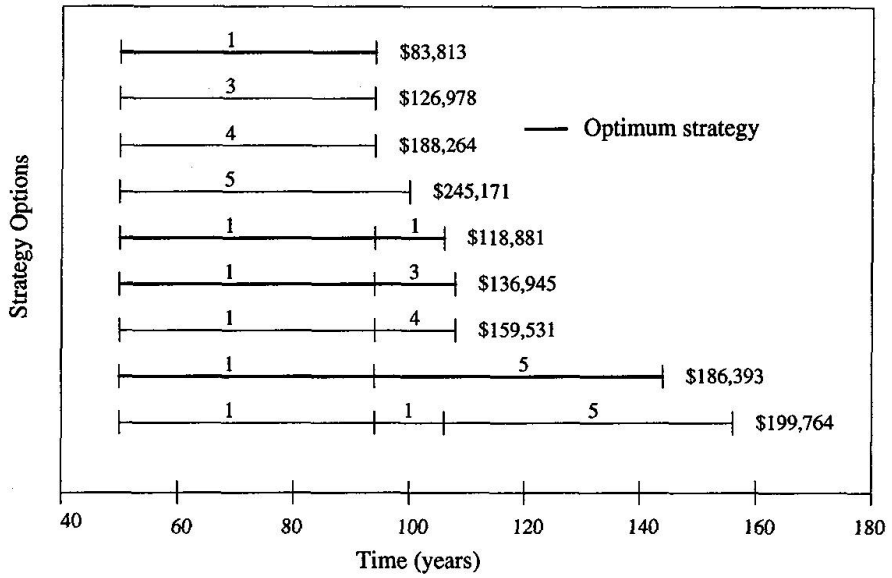

Fig. 3 Strategy options and associated costs

The reliability of a structure can be improved by increasing the capacity of the members, reducing the demand on the structure, or reducing the uncertainty in the random variables. In general, many uncertainties are site specific and if a structure already exists, these uncertainties are lower than those at the design stage [12]. By conducting tests to determine the actual strength of the steel, the unit weight of the concrete, the live-load traffic pattern, the girder distribution factors, or the thickness of the asphalt, the results may allow the subjective uncertainties to be reduced, or even eliminated, and should at least improve the knowledge of the mean value and degree of dispersion of the random variables. A sensitivity analysis of the random variables would help indicate which tests would produce the greatest benefit. This study, however, is limited to updating the effects of the time-dependent deterioration and updating the chosen deterioration models.

3. Updating the system reliability from the biennial visual inspections

In the United States, all bridges in the National Bridge Inventory (NBI) must be inspected every two years. The results are reported to the Federal Highway Administration (FHWA) and are maintained in a national data base. The minimum reporting requirement is to provide a condition state which ranges from 9 (excellent condition) to 0 (failed condition) for the bridge deck, superstructure, and substructure. As bridge management has improved over the past two decades, many states have adopted bridge management systems and more detailed inspections which provide much more information about an individual bridge. The PONTIS Bridge Management System [4] has been adopted by many states and assigns condition ratings to many elements of a bridge. These bridge elements incorporate components such as railings, joints and decks; types of materials such as concrete, steel, or timber; and other relevant information such as protected or unprotected decks, open or closed girders, and painted or unpainted stringers.

In the PONTIS system, each bridge element is visually inspected by a trained inspector and classified into one of five condition states, although some elements have fewer condition states. The five condition ratings for Element 107: Painted Open Steel Girders [4] are shown in Table 1. Updating the reliability of a bridge based on visual inspections is only possible if the conditions states are specific and quantifiable. The condition states in Table 1 rely on rust codes *R1* through *R4* to quantify the percent section loss.

CS	Description	Rust Code
1	No evidence of active corrosion. Paint system is sound and protecting the girder.	-
2	Slight peeling of the paint, pitting, or surface rust, etc. No section loss.	light *R1*
3	Peeling of the paint, pitting, surface rust, etc. No section loss.	*R1*
4	Flaking, minor section loss (<10% of original thickness).	*R2*
4	Flaking, swelling, moderate section loss (>10% but ≤ 30% of the original thickness). Structural analysis not warranted.	*R3*
5	Flaking, swelling, moderate section loss (>10% but ≤ 30% of the original thickness). Structural analysis is warranted due to location of corrosion on the member.	*R3*
5	Heavy section loss (>30% of original thickness), may have holes through the base metal.	*R4*

Table 1. *CDOT suggested Condition State (CS) ratings for Element 107: painted open steel girders [4]*

The location of the damage also must be known. A segment-based inspection first proposed by Renn [10] is used here where the location of all damage on the structure is identified. On the simple-span Bridge E-17-AH, for example, the corrosion near the supports affects the area of the web which reduces the shear capacity of the girder. The corrosion in the center of the girder reduces the plastic section modulus which is critical to the moment capacity. Furthermore, identifying whether the damage is on an exterior, interior-exterior, or interior girder also affects the system reliability.

The parameters of random variables cannot be obtained directly from a visual inspection. Some assumptions must be made regarding the accuracy of the results and quality of the information provided by the inspectors. This study assumes that condition state deterioration over time is linear and that the deterioration intensity is normally distributed. It is further assumed that when a bridge element is at the halfway point of a specific condition state, the mean value of the normal distribution is at the halfway point of the condition state definition (see Fig. 4).

The standard deviation is determined by the assumed quality of the inspection program. If the inspector is believed to be correct 90% of the time when the member is at the halfway point of the condition state, then 90% of the values in the normal distribution will be within the values prescribed by the condition state. To make this assumption conservative, the condition state is assumed to begin at the halfway point and shifts progressively to the right as shown in Fig. 4. If the element remains in the condition state longer than expected, the distribution will remain at the far right position until an inspection reveals a switch to the next condition state. The exception will be for the first and final condition states where a lognormal distribution is used.

This study considered three different qualities of inspection programs, A, B, and C, where the inspectors were provided the correct rating 95%, 85%, and 75% of the time, respectively. The quality of the inspection program was determined based on seven criteria [5] which included inspector training, a quality assurance program, and inspector experience. The density distributions associated with condition states 1 through 5 for Inspection Category A and Element 107 as listed in Table 1 are shown in Fig. 5. Condition states 1, 2, and 3 were modified to reflect section losses of 0-2%, 0-5%, and 0-10%, respectively. Once the parameters of the random variables which describe the percent section loss for the corroding steel girders are defined, the area of the web and the plastic section modulus at the time of inspection can be computed. With the revised shear and moment capacities of the girders, the updated reliability of the bridge girders is computed. Assuming linear condition state deterioration over time, the future performance of the structure is predicted.

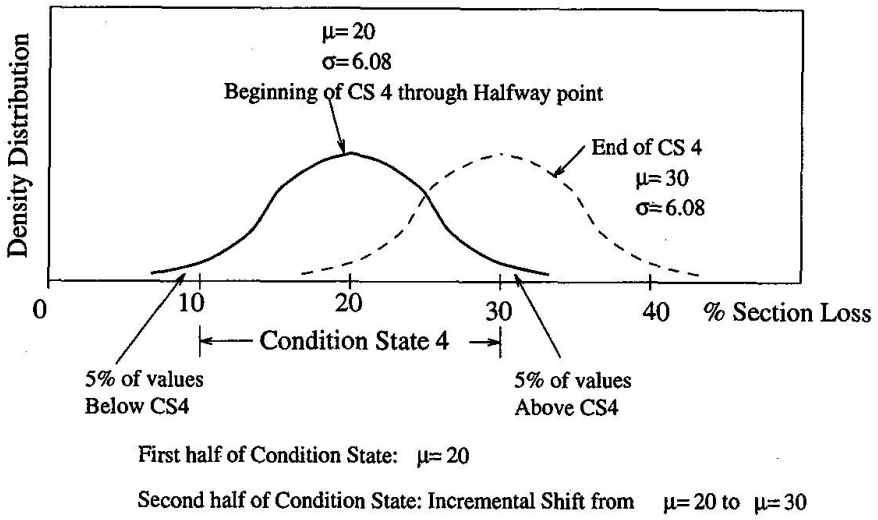

Fig. 4 Density distribution of deterioration for Element 107 in Condition State 4 when inspectors are correct 90% of the time.

Unfortunately, an update of the deck or the superstructure was not possible based on a visual inspection. The PONTIS inspection was only able to report the number of cracks, degree of efflorescence, and percentage of surface spalls. While this information is valuable for assessing the general surface condition of the deck or the pier cap, the information was not sufficient to infer the randomness of the section loss in the corroding steel reinforcement embedded in the concrete. A series of NDE inspections are needed to update the reliability of the deck.

4. Reliability updates based on Non-Destructive Evaluation (NDE) methods

While the biennial visual inspections evaluate the entire bridge, a program of NDE tests focuses on particular defects in specific areas. The tests must be selected to provide the relevant information needed to update the reliability. In this study, the thickness of the girder flanges is measured using calipers or a micrometer to obtain actual section loss. For the deck, half-cell potential tests provide the degree of active corrosion and allow the corrosion initiation time T_I to be updated. The rate of corrosion r_{corr} is then assessed using three-electrode linear polarization (3LP) test results. Because these tests were never actually conducted on Bridge E-17-AH, the inspection results from other similar structures were applied to this bridge to illustrate the updating process.

4.1 Thickness of the girders

Thickness readings on the girders were taken at numerous locations on the girders after 15, 30, and 55 years of service. The mean and standard deviation of the corrosion depth d_{corr} (in mm) were established for each type of girder (interior, interior-exterior, and exterior) for each inspection. The same format as the original deterioration model was used where time t is in years :

$$d_{corr} = A_0 t^{A_1} \tag{1}$$

The corrosion parameters A_0 and A_1 were computed by a curve fit through the data points, producing the following results:

$$d_{corr:\ exterior} = 0.13218\ t^{0.595478}$$
$$d_{corr:\ int.-ext.} = 0.12151\ t^{0.568652}$$
$$d_{corr:\ interior} = 0.03015\ t^{0.690171}$$

A comparison of the revised corrosion model with the original corrosion model [1] reveals that the actual rates of corrosion were slightly higher than predicted for the exterior girders, slightly lower than predicted for the interior-exterior girders, and almost the same for the interior girders. The inspection results produced a smaller standard deviation of thickness loss for all types of girders. This reduced uncertainty in thickness loss improves the reliability of the girders.

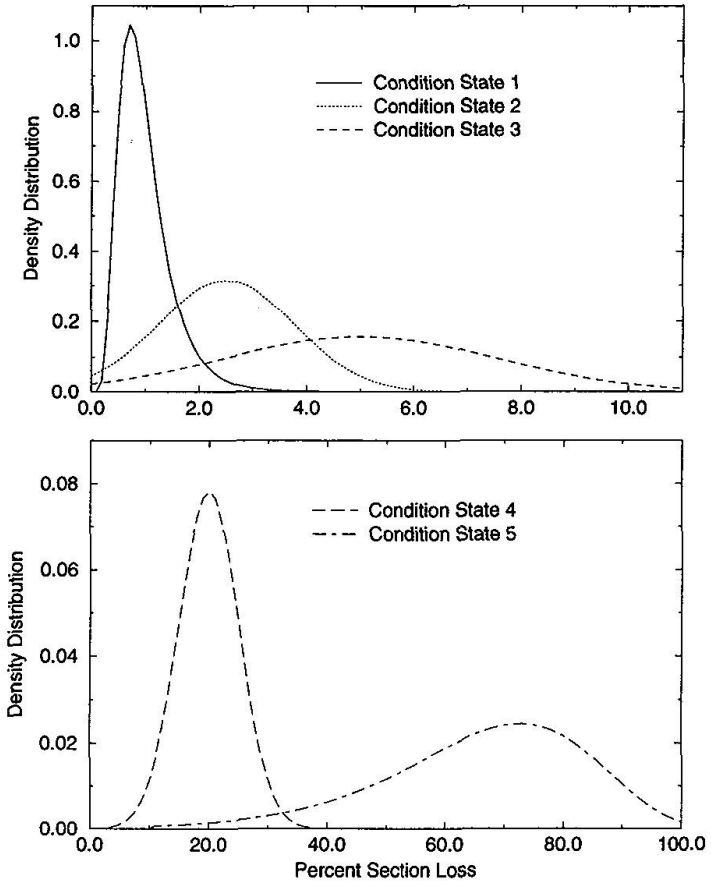

Fig. 5 Density distributions associated with Condition State (CS) ratings CS1-CS5 for Element 107: painted open steel girders, Inspection Category A

4.2 Section loss in the deck reinforcement

The half-cell potential test is conducted to obtain the percentage of the deck experiencing active corrosion. The half-cell potential survey measures the electrical potential difference between a standard portable copper-copper sulfate half-cell placed on the surface of the concrete and the embedded reinforcing steel. A potential reading more positive than -0.20 volts indicates a 90% chance of no active corrosion at the point the reading is taken. A reading more negative than -0.35 volts indicates a 90% chance that active corrosion in underway. Readings between these values are considered uncertain. By plotting a cumulative distribution of the half-cell readings throughout the deck and making a linear approximation in the uncertain range as shown in [6], the percent of the deck which is damaged can be assessed. By performing the test at several points in time, the chloride initiation time and its updated distribution can be determined as detailed by Estes [5]. In this study, the updated initiation time T_I was :

μ_{T_I} = 49.0 years and σ_{T_I} =15.0 years.

The original deterioration model predicted :

μ_{T_I} =19.6 years and σ_{T_I} =7.5 years.

While the half-cell potential test indicates if active corrosion has begun, the corrosion rate determines the amount of section loss in the reinforcing steel which results in diminished moment capacity and reduced reliability. The three-electrode linear polarization test (3LP) uses polarization resistance to determine the amount of electrical current flowing in actively corroding reinforcement. If a large flow of current is required to cause a specific change in electrical potential, the bar is corroding at a high rate. Conversely, if a small current flow is needed to cause the same change in potential, the bar is corroding more slowly. These current readings can be converted to corrosion rates as described by Clear [2].

Using current readings taken at 38 locations on the structure and using only those readings where the half-cell potential was more negative than -0.35 volts, the updated parameters of the corrosion rate r_{corr} for the embedded deck reinforcement are :

$\mu_{r_{corr}}$ = 48.5 μm/yr and $\sigma_{r_{corr}}$ =29.9 μm/yr.

The values for r_{corr} from the original deterioration model [11] were :

$\mu_{r_{corr}}$ =50.7 μm/yr and $\sigma_{r_{corr}}$ =5.8 μm/yr.

The mean value of the corrosion rate is only slightly less than the original model but the standard deviation is about five times higher. Contrary to the expected result from [12] where testing is expected to reduce the uncertainty, these test results represent an exception where inspection results provide greater uncertainty in a random variable. With revised values for the corrosion initiation time T_I and the rate of corrosion r_{corr}, the reliability of the slab can be updated.

4.3 Reliability update of the bridge

Using the results of NDE inspections, the reliability of the girders, the deck, and ultimately the system are updated. Using the same repair options listed earlier, Fig. 6 shows the results of Option 1: Replace the Deck. Fig. 6 can be compared to Fig. 2 which showed the time-dependent reliability of the bridge components and bridge system when the deck was replaced twice using the original deterioration models. Despite the updated inspection results, the figures are quite similar, except for the reliabilities with respect to girder shear. The girder reliabilities with respect to moment are close to the original model. The moment capacity is dependent on the plastic section modulus which is less sensitive to the small changes in the thickness loss. In Fig. 6, the slab is replaced at year 52 and year 98, and at year 108, a slab repair is no longer sufficient to raise the system reliability above β_{min}=2.0.

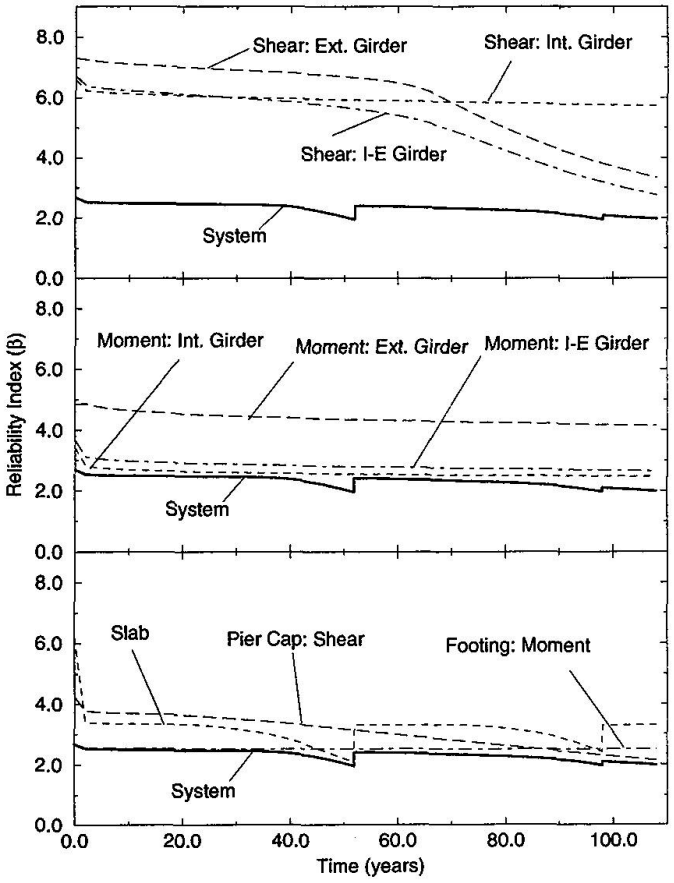

Fig. 6 Updated results of repair option 1 on Bridge E-17-AH using simplified series-parallel model requiring the failure of three adjacent girders

With regard to the reliability of the system, the girder reliabilities do not dominate the system. The reduced girder corrosion rate uncertainty improves the reliability of the individual girders, but has little to no effect on the system. The slab, which is deteriorating more rapidly than the other critical failure modes, eventually dominates the reliability of the system. The effects of longer chloride initiation time T_I and increased uncertainty in the corrosion rate r_{corr} offset each other. As a result, the minimum system reliability β_{min} =2.0 is violated after 52 years of service, which is very close to the 50 years of service in the earlier model. Again, accounting for all relevant repair possibilities and using a discount rate of 2%, Fig. 7 shows all feasible strategy options and their associated costs which can be compared to Fig. 3 using the original model.

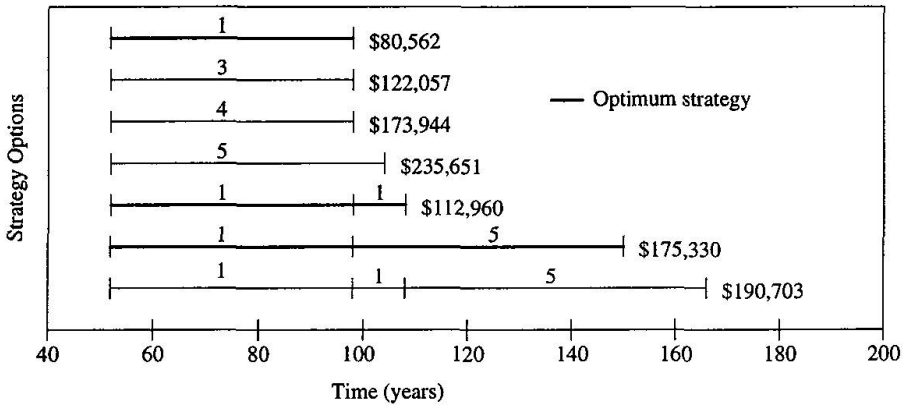

Fig. 7 Updated strategy options and costs (2% discount rate) for Bridge E-17-AH using simplified series-parallel model requiring the failure of three adjacent girders

As a result, the updated optimum strategy is as follows: for a life of 52 years, no action should be taken; for 52-98 years, replace the deck at year 52 ($80,562); 98-108 years, replace the deck at year 52 and replace the deck again at year 98 ($112,960); and after 108 years, replace the slab at year 52 and replace the bridge at year 108 ($175,330). Updated inspection results would not always produce such minor changes in strategy. The lack of change in this update is due to the compensating differences in the deck results where the positive effect of an increased chloride initiation time was offset by a more uncertain corrosion rate. If the slab had been deteriorating more slowly and the girders more rapidly than the model suggested, then the updated lifetime bridge repair strategy would have been quite different.

5. Concluding remarks

Using Colorado State Highway Bridge E-17-AH, this study illustrated how system reliability methods can be used to optimize the lifetime repair strategy while minimizing total cost and maintaining a prescribed level of system reliability. Because the initial strategy is based on assumptions that must be verified over the life of the structure, inspection results can be used to update the reliability of the structure and the repair strategy. With some reasonable assumptions, the biennial visual inspections can be used, but often the information provided is not sufficient or the condition states are not well enough defined to update the reliability. The reliability update of a structure can be completed with much greater confidence if specific NDE inspection techniques are used to provide the relevant information. In this case, thickness tests, half-cell potential readings, and three-electrode linear polarization (3LP) methods were used to update the reliability of the deck and the girders.

With the relevant NDE inspection techniques identified, the next step is to determine the optimum number and timing of these inspections over the life of the structure to minimize the life-cycle cost. As an example, Estes [5] uses a given deck structure and optimizes the number of lifetime inspections and their intervals for the half-cell potential test. There has been tremendous progress in applying reliability-based methods to optimize bridge management. As reliability theory has become better understood and accepted, the trend in research has moved toward more realistic and practical applications [7, 8]. This study is just one example of a reliability-based application which improves the life-cycle cost analysis of bridges.

Acknowledgments

This material is based upon work partially supported at the University of Colorado by the United States National Science Foundation under Grant Nos. CMS-9319204, CMS-9506435, CMS-9522541, and CMS-9522166. This support is gratefully acknowledged. Also, the support from the U.S. Army for the first author is gratefully acknowledged. The results, opinions and conclusions expressed in this paper are solely those of the authors and do not necessarily represent those of the sponsors.

References

1. ALBRECHT, P., NAEEMI, A.H. Performance of Weathering Steel in Bridges, National Cooperative Highway Research Program, Report 272, 1984.
2. CLEAR, K.C. "Measuring Rate of Corrosion of Steel in Field Concrete Structures." Transportation Research Record 1211, Transportation Research Board, National Research Council, Washington D.C., 1992.
3. CDOT: Colorado Department of Transportation. 1994 Cost Data, Cost Estimates Unit, Staff Design Branch, Denver, Colorado, 1995.
4. CDOT: Colorado Department of Transportation. BMS/PONTIS Bridge Inspection Manual. Denver, Colorado, 1995.
5. ESTES, A.C. A System Reliability Approach to the Lifetime Optimization of Inspection and Repair of Highway Bridges. Ph.D. Thesis, Department of Civil, Environmental, and Architectural Engineering, University of Colorado, Boulder, Colorado (in progress).
6. FHWA: Federal Highway Administration, Corrosion Detection in Reinforced Concrete Bridge Structures, User Manual, Demonstration Project No. 84, U.S. Department of Transportation, Washington D.C., 1992.
7. FRANGOPOL, D.M., HEARN, G. "Managing the Life-Cycle Safety of Deteriorating Bridges," Recent Advances in Bridge Engineering (Edited by J.R. Casas, F.W. Klaiber, and A.R. Mori), CIMNE, Barcelona, 1996, 38-55.
8. FRANGOPOL, D.M., LIN, K.Y., ESTES, A.C. "Reliability of Reinforced Concrete Girders Under Corrosion Attack," Journal of Structural Engineering, ASCE, New York, 123(3), 1997.
9. NOWAK, A.S. "Load Model for Bridge Design Code", Canadian Journal of Civil Engineering, Vol. 21, No. 1, 1994, pp. 36-49.
10. RENN, D.P. Segment-Based Inspection for Load Rating Within Bridge Management Systems, Master of Science Thesis, Department of Civil, Environmental and Architectural Engineering, University of Colorado, Boulder, Colorado, 1995.
11. THOFT-CHRISTENSEN, P., JENSEN, F.M., MIDDLETON, C.R., BLACKMORE, A. "Assessment of the Reliability of Concrete Slab Bridges," Proceedings of the 7th IFIP WG7.5 Working Conference, Boulder, Colorado, April 2-4, 1996, in Reliability and Optimization of Structural Systems (Edited by D.M. Frangopol, R.B. Corotis, R. Rackwitz, Elsevier, 1996 (in print).
12. VERMA, D., MOSES, F. "Bridge Reliability - Evaluation vs. Design." Probabilistic Methods in Civil Engineering (Edited by P.D. Spanos), ASCE, New York, 1986, pp. 233-236.

Inspection of Bridges with Orthotropic Steel Decks with Particular Attention to Fatigue

J. S. LEENDERTZ
Senior Design Eng.
Min. of Transport
Zoetermeer, The Netherlands

J.S.Leendertz, born in 1948 works since 1969 in the field of steel structures for bridges and hydraulic steel structures. He is chairman of an internal working group on bridge bearings and expansion joints.

Henk v.d.WEIJDE
Head of Steel Structures
Min. of Transport
Zoetermeer, The Netherlands

Henk van der Weijde, born in 1945, works since 1967 in the field of steel structures for bridges and hydraulic steel structures. Since 1989 he is head of the steel structures department.

Henk KOLSTEIN
Senior Research Engineer
TU-Delft
Delft, The Netherlands

Henk Kolstein, born in 1952 joined Delft University of Technology in 1971. Since 1978 he has been participating in research in the field of bridge loads and fatigue of orthotropic steel bridge decks.

Summary

Structures of orthotropic steel decks, where the deck plate with open or closed stiffeners is supported by and establishes an integrated structure with the deck and crossbeams, show to be susceptible to traffic induced fatigue. This paper shows the behaviour of the stiffener to crossbeam connections in various structures in the Netherlands. The behaviour is related to the essential locations for inspection and several examples of damage in real bridges.

1. Introduction

Most bridges with orthotropic steel bridge decks have been built in the period from 30 to 10 years ago. Several of these structures show fatigue induced cracks in the locations where the stresses are governed by the traffic loads. Although the orthotropic steel decks have become relatively expensive solutions for bridges with shorter spans, they are still used in bridges with longer spans, where the dead weight must be low and for upgrading of existing bridges.

The amount of approximately 300 existing bridges with these structures in the Netherlands, controlled by the Ministry of Transport, causes the need for further investigations in order to obtain a good insight in the behaviour, the fatigue strength and the critical locations of these structures. As the critical locations for fatigue do not always coincide with the critical locations for the ultimate limit state, inspections can be more adequate and limited to specific locations.

This paper will show the common structural bridge types in the Netherlands as well as their behaviour and the way how details are addressed by the traffic loading. Essentially these structures exist all over the world. The damage of several real bridges is shown as an example.

2. Orthotropic steel deck types

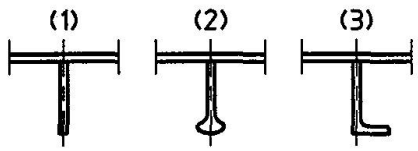

Fig. 1 Open stiffeners

The earlier orthotropic steel decks were stiffened by flats and bulbs (see Fig.1), thus allowing for spans of approximately 2.0m. The connection to the crossbeams have been featured in two ways: 1. fitted between the crossbeams; 2. continuous stiffeners passing through special cut outs eventually with additional cope holes in the crossbeams. The rather small stiffness and strength of these stiffeners caused the need for many crossbeams. A number of these crossbeams, the secondary crossbeams were supported by additional main girders, the secondary main girders. The latter were supported by the primary crossbeams that transmitted the loads to the main girders. The fabrication of these structures with many cut outs and welds was laborious and subsequently expensive. This caused the need to develop structures with less welded connections. Nowadays open stiffeners are mainly used in ferry bridges, where a low torsional stiffness of the deck is required due to the movements of the mooring ships.

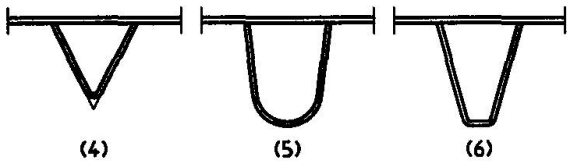

Fig. 2 Closed stiffeners

The introduction of the closed V-shaped, U-shaped and trapezoidal stiffeners as shown in Fig. 2, was a large improvement, which alloyed spans of approximately 4.0m. The secondary crossbeams and main girders were no longer needed. The amount of work involved reduced as well as the costs.

Like the open stiffeners the closed stiffeners could be fitted between or as continuous elements passing through the crossbeams. In this case the cut-out can be of close fit or being featured with an additional oval shaped cope hole or other like the "Haibach" cut out. All details showed to be susceptible to fatigue induced cracks, which resulted in world wide research to the fatigue strength of the details in order to develop data that can be used for the design of new bridges and the repair of existing structures.

Fig. 3 shows a complete overview of all types of closed stiffeners and stiffener to crossbeam connections used in the Netherlands.

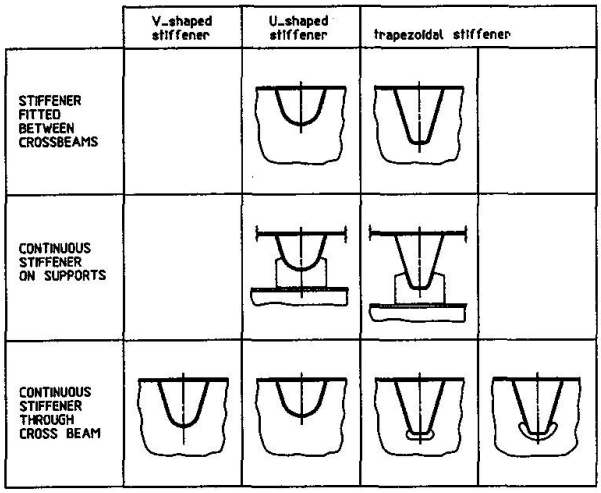

Fig. 3 Types of trough to crossbeam connection

3. Structural Bridge Types

3.1 General

In the orthotropic steel deck structures the deck plate acts together with the longitudinal stiffener. This system transmits the loads to the crossbeams. The latter transmit the loads to the main load carrying system, which can be constructed as plate girders or a box girder. The main load carrying system may be integrated in one of higher rank, such as an arch, a cable stayed structure or a suspension structure.

3.2 Structural systems

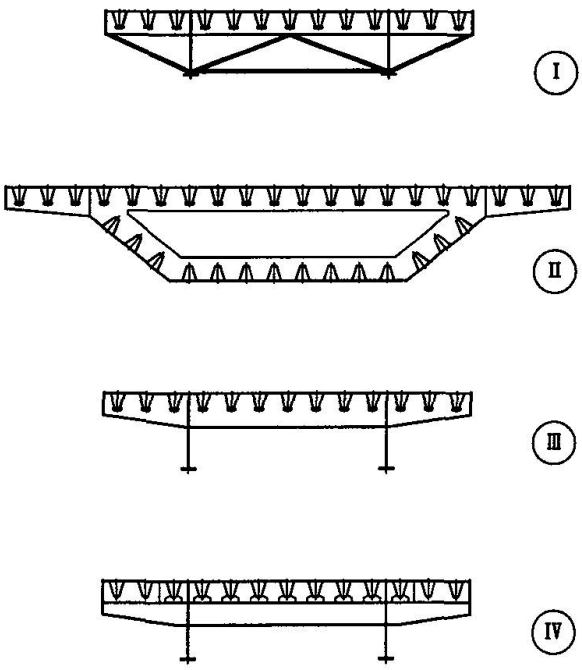

Fig. 4 Structural types of bridges

Fig.4 shows four load carrying systems. For simplicity only systems with continuous closed stiffeners are shown. Type I is a plate girder bridge with crossbeams that consists of a truss and a top cord acting as a continuous beam with short spans. The continuous beam transfers the loads by bending and shear to the truss nodes. The truss is supported by the main girders. Type II is a box girder bridge. The diaphragm of the box acts as a deep crossbeam that transfers the loads to the inclined and vertical webs of the box girder. Type III is a conventional crossbeam with cantilevers that are supported by the main girders. Type IV is an I-shaped crossbeam that receives the loads from the supports of the closed stiffeners. The shear connections in the cantilever sections cause a rotational spring using the axial stiffnesses of the deck plate and the I-beam and a lever arm. This is called the "Floating Deck Structure" and is used in a few bridges in the Netherlands [1]. It has been developed for its easy of assembly.

3.3 Structural behaviour

In addition to the in plane shear and bending that is generated by the loading of the crossbeams, all structures are subjected to out of plane rotations, caused by the deflection of the stiffeners. In the combination effect the contribution from "in plane" and "out of plane" behaviour differs from type to type and depends strongly on the structural features.

4. Stiffener to crossbeam connections

4.1 Open stiffeners

Open stiffeners are fitted between the crossbeams or are continuous. The first type is sensitive for eccentricities related to the continuous stiffener and the welded connection to the crossbeam.

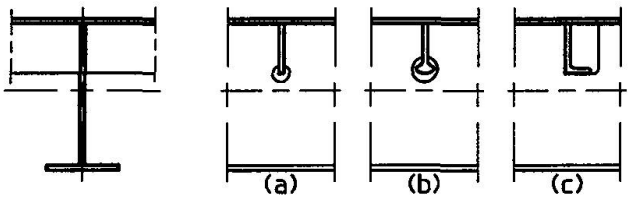

Fig. 5 Crossbeam connections with continuous open stiffeners

Because the influence lines show short distances between the zero-crossings a rather unfavourable connection is submitted to many cycles caused by the wheel loads. Fig.5 shows the connections of continuous open stiffeners to the crossbeams. In the connections shown, cope holes have been used for fitting purposes. The cope hole causes a discontinuity in the crossbeam. In Fig.5 type (a) and (b) it causes a local stress concentration, but in Fig.5 type (c) a "Vierendeel" effect with additional bending is to be expected. This effect will be explained later in conjunction with the closed stiffener connections.

4.2 Closed stiffeners

Closed stiffeners are sometimes fitted between the crossbeams, but more often they are continuous. In the latter case they may be welded all around, or passing through cut outs, eventually with additional cope holes for fitting purposes. In the past the connections with cope holes have been investigated extensively in order to analyse the fatigue strength and to optimise the shape. [2,3]

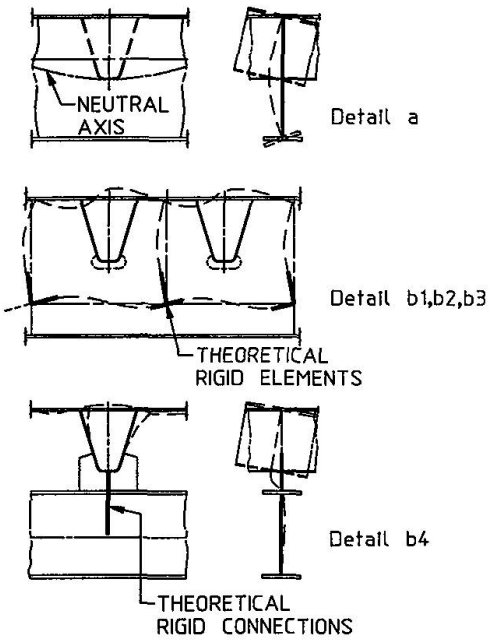

Fig. 6 Closed stiffener connections and structural behaviour

Fig.6 shows both the connections and their structural behaviour. Two groups are distinguished:

a. Troughs fitted between the crossbeams

b. Continuous troughs passing through cut outs with cope holes

Usually Group "a" connections are applied in structures with shallow crossbeams, where cut outs cause a too low shear capacity of the crossbeam. In the past, the detail with fillet welds showed many fatigue cracks. The details with full penetration welds show a much better fatigue performance.

The Group "b" connections are applied in structures with deeper crossbeams, diaphragms of Box Girder Bridges, "Floating Deck" structures. The following subdivision can be made:

"b1": Continuous troughs passing through a cut out with close fit and welded around with fillet welds;
"b2": Continuous trough passing through a cut out with an oval shape or similar;
"b3": Continuous trough passing through a cut out with additional cope holes with varying radius, the so-called "Haibach cut out" [4] or a similar shape;
"b4": Continuous trough supported by a counter-fitted support plate, welded around the bottom of the trough. Further the support is welded to an I-beam.

4.3 Mechanical behaviour of the connections

In the application of the detail "a", a discontinuity in the stiffener exists with the possibility of eccentricities. The crossbeam section remains practically unchanged. The stiffener rotations cause "out of plane" rotations in the web of the crossbeam.

The structural behaviour of the details "b1", "b2" and "b3" is the same, with minor differences.

In plane, the cut out causes a "Vierendeel Effect" if the depth of the cut out is substantially, compared to the depth of the crossbeam or diaphragm [5,6,7]. This is likely to occur if the detail is applied in Crossbeams Type I and III bridge structures (see Fig.6). Further all details are subjected to locally applied forces and a contraction effect of the bottom of the stiffener caused by bending moments at the stiffener supports [8].

Out of plane rotations are transmitted to the web of the crossbeam or diaphragm. The detail "b1" acts more rigid than the details "b2 and b3".

The detail "b4" does not participate substantially in the in plane load carrying behaviour of the crossbeam, as the shear connection between deck and I-beam caused by the trough is flexible. The out of plane rotations of the stiffeners are transmitted by bending in the support plate to the I-beam which will rotate and translate out of plane in line with the horizontal and torsional stiffness of the I-beam.

5. Crossbeam in-plane behaviour

In crossbeams with connections "b2" a significant part of the web has been removed. Consequently an "in plane" Vierendeel behaviour is generated (see Fig.7). The part between the troughs, often called the "tooth" acts as a post clamped in a continuous T-beam upside down. Below the cut outs the T-beam remains as the bottom cord. Between the cut outs the web is fully intact. Features like the presence or absence of different shaped cope holes do not change the behaviour significantly [7].

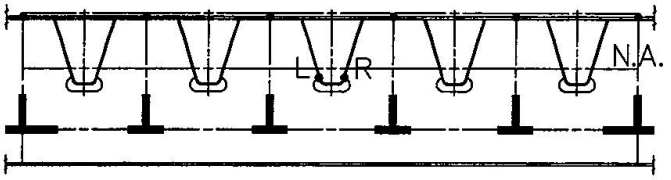

Fig. 7 Vierendeel system

Due to crossbeam bending the locations "L" and "R" translate in horizontal direction. Depending on the neutral axis of the system an elongation or compression of the distance between them, is generated. Shear forces cause relative vertical displacements and rotations in the locations "L" and "R". In [4] these phenomena have been reported for detail "b2". Further, nominal stresses for a set of beams have been calculated. These results have been combined for the locations in the beam where the interaction between shear and bending effects reaches a maximum. For easy comparison the external load introduction is ignored in these results.

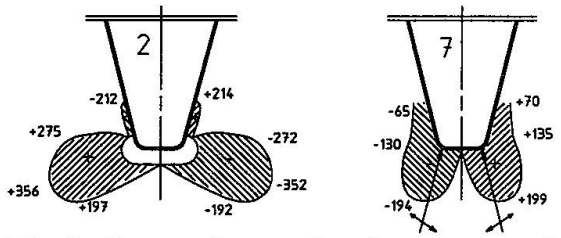

Fig. 8 Principal stress distributions around cut out and continuous weld (N/mm²)

Fig.8 shows the results of FE-analyses with for a test specimen [3,7,9] the principal stresses around the cut out for crossbeam to trough nr. 2 (detail "b2") connection and a fully welded around crossbeam to trough nr. 7 (detail "b1") connection under the same but symmetrical bending and shear loads. The model consists of shell elements, which ignores the effect of the plate and weld dimensions in the neighbourhood of the welds. The arrows show the direction of the principal stresses at a specific location. Near to the welds the stress levels reach approximately the same level, but the direction with respect to the weld is completely different. Fatigue tests on a true scale specimen [3] showed a better performance for the connection of trough nr.7.

In the "Floating Deck" structure as shown in Fig.9 [1,10], the end of the I-beam is restrained by the lever system, which generates a compression in the deck and a tension in the I-beam. The horizontal compression and tension forces at a distance a_l are balancing the bending moment M_S at the support. The normal forces in the deck and the I-beam, the rotations in the I-beam and the shear deformation in the I-beam cause the deck shifting over a distance S_h with respect to the I-beam as shown in Fig.10. Asymmetrical loads cause in some locations larger shifts S_h [10].

The shift S_h generates normal forces and bending moments in the trough web. Fig.11 shows the nominal stresses in the trough web and the deckplate caused by the shift S_h of 1mm. The shifts S_h for a set of beams of with depths are shown in [10]. Realistic values of S_h under maximum crossbeam loading vary from 0.1 - 3.3 mm. In real structures these stresses must be multiplied with a stress concentration factor in order to find the Hot Spot Stresses which are relevant for fatigue.

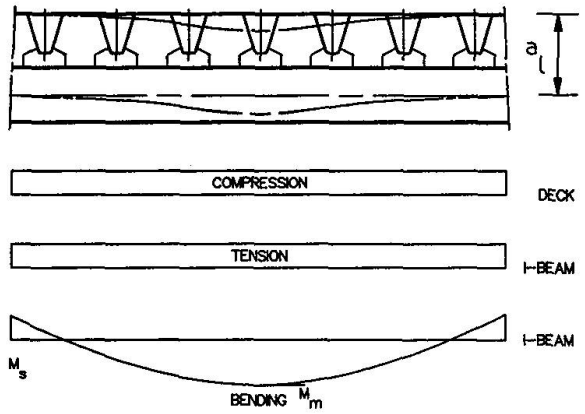

Fig. 9 Model of floating deck crossbeam

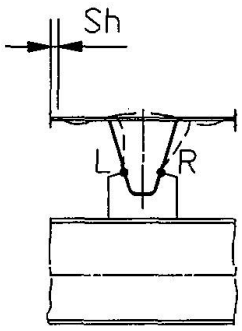

Fig. 10 Horizontal shift S_h

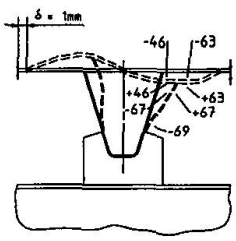

Fig.11 Stresses at a shift S_h of 1 mm (N/mm²)

It is obvious that these stresses which mainly are governed by bending effects in the deck plate and trough web, can not be neglected. The stress concentration factors related to the bottom connection are assumed to be higher than the stress concentration factors related to the trough to deck connection. If however the stresses due to the wheel loading on the deck are added, high stress amplitudes may occur due to the combination of both effects.

6. Crossbeam out-of-plane behaviour

Passing vehicles generate bending and shear in the stiffeners, which deflect subsequently and makes the supports of the stiffeners rotate (see Fig.6). The rotation of this connection causes an out of plane movement of the crossbeam web. This phenomenon takes place in all types of stiffeners. The connection "b2" has been investigated in ECSC research Phase 3 and 4. In [2,3] the fatigue behaviour has been reported for various types of stiffeners and cut outs. The fatigue strength of details "b2" has been investigated under simultaneous vertical forces with out of plane bending in the web plate. Fig.12 shows for three test specimens the stress results of FE analyses under equal vertical load and out of plane rotation.

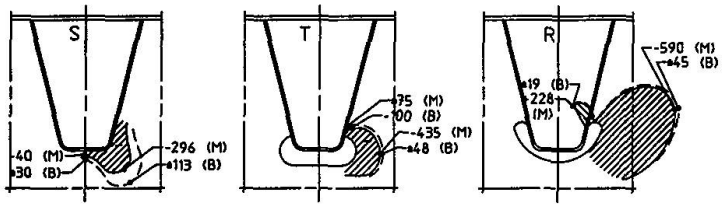

Fig. 12 Stress distributions under vertical load in combination with out of plane bending (N/mm²)

The stresses shown are the membrane stresses (M) and the out of plane bending stresses (B) for test specimens at the Stevin Laboratory (NL) as reported in [2]. The models consisted of shell elements, which means that the stresses in the neighbourhood of the trough to crossbeam connection do not include the weld and plate dimension effects [9]. Nevertheless it is obvious that in this case, the rigid support not far below the trough to crossbeam web connection causes in the detail "b1" (S) much higher bending stresses than in the details "b2" (T) and "b3" (R). The types "b1";"b2" and "b3" refer to the detail categories of Section 4.2. The tests in the Stevin laboratory showed a better fatigue strength for the type "S", if compared to the types "T" and "R". The V-shaped stiffener connection tested at TRL (UK) however showed a lower fatigue strength. The results have been reported in [2].

7. Welded details

As a simplification, most of the details used in real structures can be reduced to 2 types of welded details , those with and without cope holes, see Groups "a" and "b" in Section 4.2. The combination of relevant degrees of freedom and the critical locations can be derived from the mechanical behaviour. Fig.13 and Fig.14 show the relevant degrees of freedom and critical fatigue locations for details without and with cope holes, Groups "a" and "b", respectively. Particular attention must be paid to the relevant influence lines and the stress concentration factors related to a degree of freedom and stresses in a specific location.

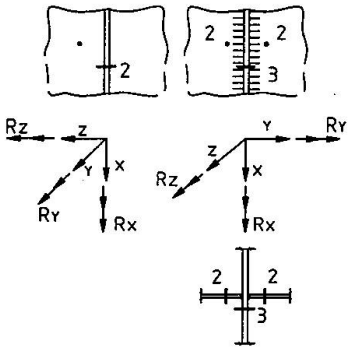

Fig. 13 Fatigue locations and degrees of freedom detail "a"

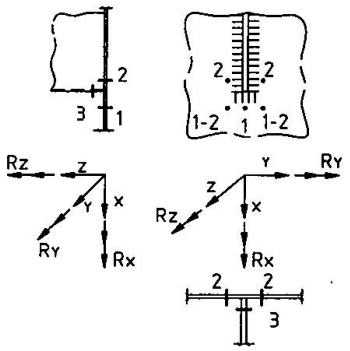

Fig. 14 Fatigue locations and degrees of freedom detail "b"

8. Combination of Effects in Critical Locations

8.1 Influence lines and transfer functions

Once the structural behaviour of the bridge structure is known, it is possible to derive the transfer functions for crossbeam loading and out of plane rotations. The transfer functions that govern the stresses in the above mentioned locations depend on the in plane stiffness (shear and bending) of the crossbeam vs. the bending stiffness of the deck structure.

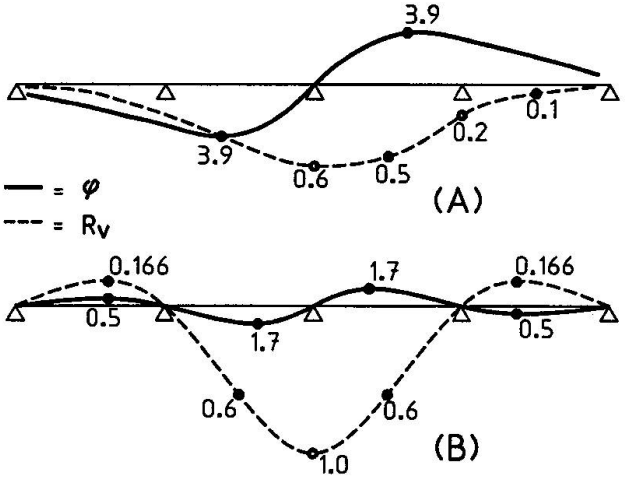

Fig. 15 Influence lines for stiffener support rotations (f) and reactions (R_v)

Fig.15 shows the influence lines for rotations (ϕ) and crossbeam loading (R_v) of the middle trough stiffener support due to wheel loads. Lines (A) show the results for more flexible crossbeams and a (B) for more rigid crossbeams. Rigid crossbeams show higher loading than flexible crossbeams, but the amount of cycles under unit loads is higher. This effect applies as well for vehicle loads.

Flexible crossbeams show larger rotations, but a smaller amount of cycles than rigid crossbeams. It may be expected that in many cases open stiffeners will tend to have an influence line of type (B) which applies for closed stiffeners in box girder bridges too.

Closed stiffeners near crossbeam mid-span in plate girder bridges will act according a line between (A) and (B), depending on the vertical stiffness of the crossbeam. Near the supports they will tend to behave like (B).

8.2 Evaluation

Combining the knowledge of the structural bridge type behaviour, the susceptible details can be classified as shown in Table 1. (details type "a", not considered). The damage in real bridges can be compared to the detail classification.

SUSCEPTIBLE LOCATIONS				
Stiffener Type	Structural Bridge Type	Mechanism	"b"	'3'
1. Open	I. Plate Girder Crossbeam Truss	Out of Plane dominant	"b"	'3'
2. Closed	II. Box Girder	Out of Plane with In Plane Support	"b"	'1-2','3'
	III. Plate Girder Crossbeam with Cut Outs	a. Crossbeam Midspan Out of Plane with In Plane Support	"b"	'1-2','3'
		b. Crossbeam Support Out of Plane with In Plane Support and Vierendeel Effects	"b"	'1','1-2','3' particularly under wheel tracks
	IV. Plate Girder Floating Deck	a. Crossbeam Midspan Out of Plane with Support and Shift Effects	"b"	'1','3' particularly under wheel tracks
		b. Deck Combination of Shift Effect and External Loads	not classified	Longitudinal deck to stiffener weld under wheel tracks

Table 1

9. Damage examples

9.1. Open stiffeners

In two plate girder bridges with open stiffeners and truss diaphragms cracks have been found in the stiffener to crossbeam connections [11]. Here the bulb stiffeners pass through circular cut outs as shown in Fig.5(b).

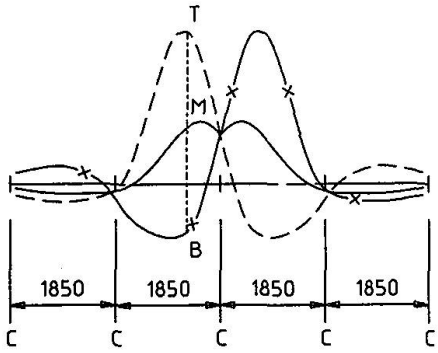

Fig. 16 Influence line stresses outer side web plate location "P"

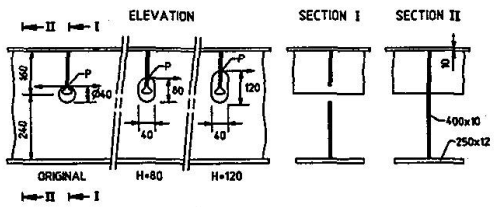

Fig. 17 Original detail and investigated cope holes and stresses for location "P"

Fig.16 shows for a 1kN wheel load the influence lines for the stresses in location "P".

Fig.17 shows the investigated details and stress locations. The out of plane bending of the crossbeam web showed to be of large importance. Two alternative cut outs with a larger depth have been investigated. The H=80 cut out has been selected as solution for the repair, because it showed a reduction of the stress amplitudes to 78% and proved to have the required shear capacity.

9.2 Closed stiffeners in structural bridge type II

In one box girder bridge cracks in the corrosion protection have been found in location '1-2' [11]. This may indicate that future cracks will occur in the steel structure.
If so the damages can be related to test series ECCS Phase 3 [2], small test specimens.

9.3 Closed stiffeners in structural bridge type III

In two plate girder bridges a number cracks have been found in location '3' [11]. The amount of defects was in line with the increasing shear force along the crossbeam towards the main girder. The damages can be related to the test series ECCS Phase 3 [2], small test specimens and Phase 4, large test specimens [3] and the analyses of the structural mechanisms as described in Heron 3 1995 [7].

The welds have been replaced without a modification of the detail. Special attention has been paid to the execution aspects.

9.4 Closed stiffeners in structural bridge type IV

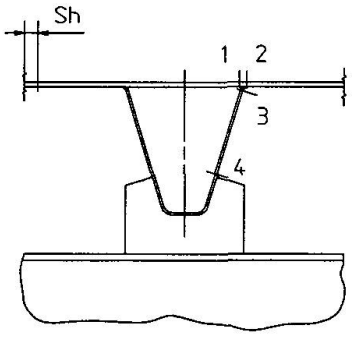

Fig. 18 Relevant locations for fatigue

In two bridges with the "Floating Deck" structure [1,9] some cracks were found in the longitudinal trough to deck weld (location 3) in the crossbeam neighbourhood of the crossbeam during a resurfacing operation [11]. Fig. 18 shows the relevant locations for fatigue which relate to the stresses in Fig 11. In the inspected bridges the deck plate had a thickness of 10 mm. No other cracks were found. The lack of time and the obtained insight in the mechanism led to the decision that the crack and the original weld were ground and replaced by a weld of 80% penetration, which had to be made in an overhead position. During repair the bridge was closed for all traffic.

10. Concluding remarks

- In general, the cracks found during inspections are in line with the described susceptible locations.
- The structural behaviour of the crossbeams and deck has been investigated in analytical methods and by Finite Element Models with shell elements. More specific analyses including the weld geometry and plate thickness will be needed.
- The fatigue strength of the various details has been investigated but not yet for all possible loading combinations related to the degrees of freedom.
- The stress concentration factors and their influence have not yet been fully investigated.
- The appropriate influence lines for crossbeam loading and rotations including the crossbeam flexibility must be linked to the vehicle spectrum.

Acknowledgement

The authors wish to thank their colleagues of the Ministry of Transport, Public Works and Water Management for their fruitful co-operation.

References

1. YPEY E. New Developments in Dutch Steel Bridge Building. IABSE Congress, Amsterdam 1972.

2. BRULS; BEALES; BIGNONNET; CARAMELLI; CROCE; FROLI; JACOB; KOLSTEIN; LEHRKE; POLEUR; SANPAOLESI Measurements and Interpretation of Dynamic Loads on Bridges (3). Commission of the European Communities. Report, Brussels 1991.

3. BRULS; CARAMELLI; CUNNINGHAME; JACOB; KOLSTEIN; LEHRKE; LE PAUTREMAT Measurements and Interpretation of Dynamic Loads on Bridges (4), Commission of the European Communities. Report, Brussels 1995.

4. HAIBACH E., PLASIL I. Untersuchungen zur Betriebsfestigkeit von Stahlleichtfahrbahnen mit Trapezhohlsteifen im Eisenbahnbrückenbau. Der Stahlbau 9, 1983.

5. FALKE J. Zum Tragverhalten und zur Berechnung von Querträgern orthotroper Platten. Diss. Technische Universität Braunschweig, 1983.

6. LEENDERTZ J.S.; KOLSTEIN M.H. Numerical Analyses of the Trough to Crossbeam Connections in Orthotropic Steel Bridge Decks. Proceedings Nordic Steel Conference, Malmö 1995.

7. LEENDERTZ J.S.; KOLSTEIN M.H. The Behaviour of Trough Stiffener to Crossbeam Connections in Orthotropic Steel Bridge Decks. Heron Volume 40, Delft 1995.

8. WOLCHUK R.; OSTAPENKO A. Secondary Stresses in Closed Orthotropic Deck Ribs at Floor Beams. ASCE Journal of Structural Engineering, Volume 118, No.2, 1992.

9. KOLSTEIN M.H.; WARDENIER J.; LEENDERTZ J.S. Fatigue Performance of the Trough to Crossbeam Connections in Orthotropic Steel Bridge Decks. Nordic Steel Conference Malmö 1995

10. LEENDERTZ J.S.; KOLSTEIN M.H. Structural Types and Endurance Aspects of Crossbeams in Steel Orthotropic Plate Girder Bridges. ICASS Proceedings, Hong Kong 1996.

11. MIN. OF TRANSPORT, PUBLIC WORKS and WATERMANAGEMENT Various Inspection Reports. Not published

Interaction between Planning, Execution and Evaluation of Tests

Peter TANNER
Research Engineer
Inst. of Const. Science (IET-CSIC)
Madrid, Spain

A graduate of ETH Zurich, in 1989 Peter Tanner joined ICOM (Steel Structures) at EPFL where he worked in the fields of fatigue and fracture mechanics. Since 1992 he has worked with consultants in Madrid. Presently, at IET-CSIC, he is performing research into durability of concrete marine structures and reliability of existing structures

Summary

The evaluation of a riveted wrought iron bridge from the last century is described. The case study concentrates on the planning of the test and inspection programme for the collection of site data and the introduction of this data in the structural calculations. The site data is used to calibrate updated deterministic models of action effects and resistance, applying reliability methods to a simple structural model. Based on the updated action effects and resistance, the required strengthening of structural members can be established through a deterministic analysis of a refined structural model.

1. Introduction

When assessing the structural safety of an existing structure, the information is different from that available during design because many characteristics may be measured from the structure under consideration which, at the time of its design, were just anticipated quantities. The level of accuracy for the load and resistance models, which are needed for the assessment, can be increased for example by visual inspection, material testing or field testing. It is always possible to improve these models by collecting more data about the assessed structure. However, the updating of information by collecting site data may result expensive, time consuming or even ineffective if the choice of the test programme is not made to suit the characteristics of the structure under investigation and if the updated information can not easily be introduced in the calculation models used for the assessment. Tests should therefore carefully be planned, executed and evaluated.

This paper deals with the evaluation of the structural safety of a 100 year old wrought iron truss-girder bridge. The relationship between planning, execution and evaluation of tests is emphasized.

2. Description of the bridge

The bridge investigated crosses the Duero river in Zamora, Spain, and was built around 1895. It is a continuous riveted wrought iron truss-girder bridge over five spans (43.2, 54, 54, 54, 43.2 m) with a total length of 248.4 m. The two main girders beams consist of parallel horizontal U-section members and crossed diagonals (Figure 1).The platform is composed of a wrought iron framework which supports the deck, consisting of a wrought iron sheeting, a sand fill and an asphalt layer. At present, the main girder bottom U-section members are affected by severe corrosion due to poor detailing and reduced maintenance in the past. For this reason, a bridge evaluation is to be initiated.

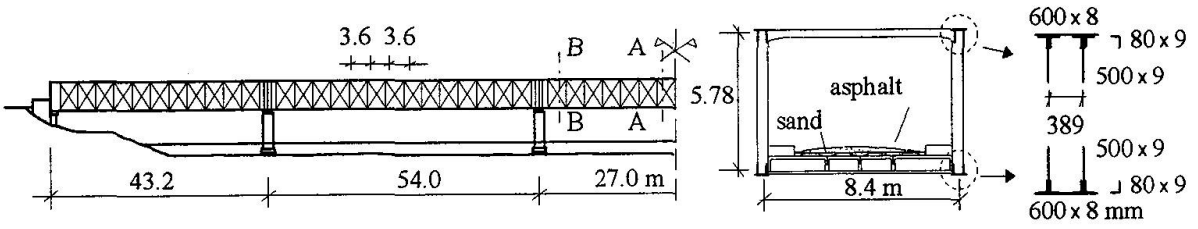

Fig.1 View and cross-section of the investigated truss bridge

3. Evaluation procedure

The assessment of the structural safety is carried out applying a staged procedure. Figure 2 shows the concept of the staged evaluation procedure and its relation to the collection of site data by inspection, material- and field testing.

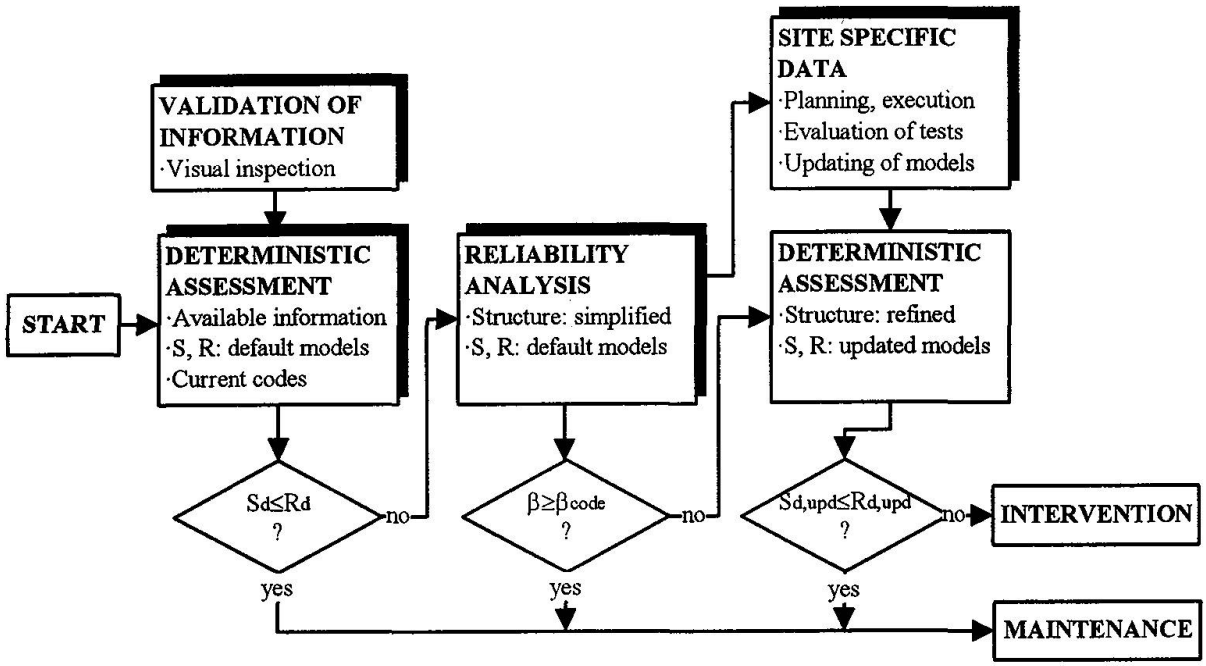

Fig.2 Staged evaluation procedure and its relation to the collection of site data

In a first step, a preliminary deterministic assessment is carried out, using the verification criteria defined in the current Spanish bridge design code [1]. For this, the calculation models are based on the available information about the structure, validated by visual inspection. No further evaluation is necessary for the members for which structural safety is verified in this first step.

For the most critical area, identified in the first step, a simplified structural model can be established that permits a reliability analysis using default probabilistic models of action effects and resistance. If the structural safety of this area is not verified, further evaluation is possible based on improved load and resistance models. The improvement of these models is possible through the collection of site data. The aforementioned reliability analysis aids the planning of site data collection: From the results it can be deduced which parameters can be most effectively updated.

The site data can be used to calibrate updated deterministic models of action effects and resistance. For the calibration, reliability methods are applied to the simplified structural model mentioned above. The updated deterministic models of action effects and resistance are then used for a detailed deterministic assessment using a more refined structural model.

For the structural members for which safety is not verified by deterministic assessment with updated models, a reliability analysis could be used for a more accurate assessment of structural safety. However, due to the large number of different structural elements, nodes and riveted connections, a full reliability analysis is not considered viable for the investigated bridge. An intervention must be planned for the members for which safety is not verified by any of the aforementioned assessment methods.

4. Collection of site specific data

4.1 Critical areas

4.1.1 Validation of information

The available information about the structure is validated by a first visual inspection before carrying out the preliminary deterministic assessment. The most important findings can be summarised as follows:

- Important eccentricities exist at main girder nodes, not visible from the geometry of the original plans (Figure 3).
- Advanced global corrosion of the truss girder bottom U-section member can be observed, facilitated by its channel like geometry. A large number of holes with dimensions of the order of 20·40 cm exist (Figure 3).
- Buckling is found of the slender "web plates" (with a height to thickness ratio of 55 and a free edge as can be seen from Figure 1) of top and bottom U-section compression members.
- Fatigue cracks in truss top lateral sway frames are observed, spreading out from rivet holes (this finding is important with a view to the evaluation of fatigue safety and the planning of maintenance and inspection strategies [2, 3]; however, fatigue and brittle fracture are not further considered in the present paper).
- The foundations are in a very good state.

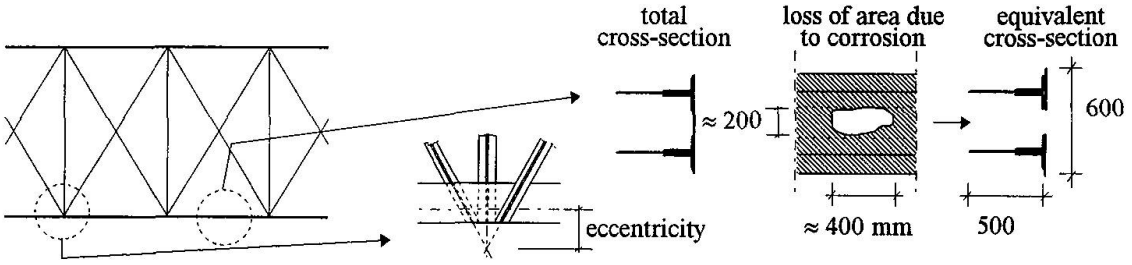

Fig.3 Validation of information

4.1.2 Preliminary deterministic assessment

Structural safety is evaluated by applying the verification criteria defined in the relevant design standards. The action effect, S, is calculated by using actions and load factors according to [4] and by introducing in the structural model the aforementioned eccentricities at main girder nodes. The corrosion of the truss girder bottom U-section members is taken into account by adopting an equivalent cross-section according to Figure 3 for the calculation of the resistance, R. Information about the material properties of wrought iron is available from literature [2], and resistance factors are adopted from [1]. The structural safety can be expressed by a rating factor, r:

$$r = \frac{R / \gamma_R}{S_d} \tag{1}$$

R resistance
S_d design load effect

γ_R resistance factor (=1.10)

If r is greater than or equal to 1.0, the investigated member or connection reaches the required structural safety level according to the Spanish codes. If the rating factor is less than 1.0, then structural safety is not verified and there is a need to perform a more accurate evaluation. The preliminary deterministic assessment reveals that the governing elements regarding load carrying capacity of the bridge are the top and bottom U-section compression members at midspan and over the piers, respectively (sections A-A and B-B, respectively, in Figure 1). Quite a number of these elements do not reach the required safety level. The minimum value for the rating factor r, equal to 0.57, is obtained for the main girder top U-section member at midspan (Figure 1, section A-A).

4.2 Importance of different variables for safety

4.2.1 Simplified structural model

Once the compression members at midspan and over the piers are identified as the critical areas, it can be assumed that the structural behaviour is brittle and that there is no significant system redundancy. Therefore, the failure of the most critical member leads to the failure of the system. Consequently, the failure probability for the bridge is governed by the failure probability of the most critical member [5].

Due to the aforementioned eccentricities at main girder nodes, the most critical member is subject to combined bending and axial compression. Although the "web plates" of the U-section are slender (Figure 1), the governing combination of bending moment, M, and axial compression, N, which defines the Ultimate Limit State of the critical member, leads to a loss of stiffness due to plate buckling of the order of only 18.5%. Therefore, the ends of the member are not free to rotate in the plane of buckling (plane of the girder, Figure 4). According to [1], the buckling length, l_p, of a truss girder top compression member corresponds to the length of a "pin ended" member which has the same buckling resistance. In the present case it can be assumed that l_p = 0.9·l. The reliability analysis can now be carried out for the simplified structural model, consisting of a "pin ended" member with a length of 0.9·l which is subject to combined bending and axial compression according to Figure 4.

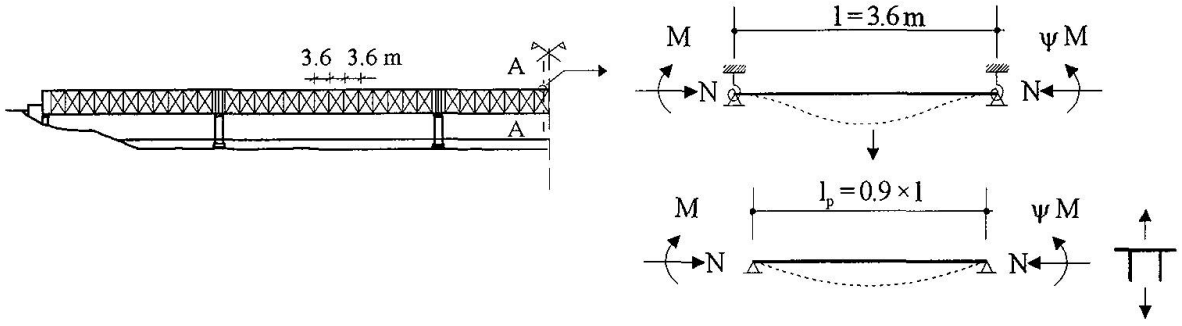

Fig.4 Simplified structural model for reliability analysis

4.2.2 Reliability analysis

Basic variables which are considered for the assessment of structural safety are associated with uncertainty. The safety of a structure can therefore be measured in terms of, for example, its reliability which takes account of uncertainty and is represented by a probability of failure.

The safety of a structure is expressed in terms of the basic variables by the Limit State Function (LSF). The most simple LSF defines safety as the requirement that resistance, R, is greater than or equal to the total action effect, S:

$$R - S \geq 0 \qquad (2)$$

The probability of failure, p_f, is thus equal to the probability that S is greater than R.

Different numerical or analytical reliability methods exist for the analysis of structural safety. The First Order Second Moment (FOSM) method [6] introduces for example a reliability index, β, for which a direct link to the failure probability exists. Even though the FOSM reliability method only produces an estimate of failure probability, the resulting errors are small if it is used to compare the failure probabilities for a given LSF and varying basic variables. This is what the FOSM method is used for in the present study: Going out from the *axiom* that a correct application of the current codes results in a safe structure, the verification of structural safety of an existing structure consists of three steps [7]:

- Dimensioning of the existing structure according to a consistent set of codes,
- Calculation of the reliability index, β_{code}, related to the dimensions obtained in the first step, considering the parameters (mean value, standard deviation, probability distribution) of the variables assumed to lie behind the rules of codes,
- Calculation of the reliability index, β, related to the actual structure using default probabilistic models of action effects and resistance.

The structure may be considered safe if

$$\beta \geq \beta_{code} \tag{3}$$

In the case of the investigated truss bridge, in the first step the main girder top U-section member at midspan (Figure 4) is to be dimensioned according to the current codes [1, 4]. The analysis reveals that a rolled profile HEB 300 is required with a specified nominal yield strength of f_y = 235 N/mm^2. Such a main girder top member at midspan may be considered safe according to the aforementioned *axiom*.

In the second step the reliability index, β_{code}, of the above safe member is to be calculated. The LSF which is used in this reliability analysis is derived from the Spanish code [1] for the verification of structural safety of members subject to combined bending and axial compression:

$$f_y - \frac{\left(N_a + N_s + N_p + N_q\right)}{\chi\, A_{eff}} - \frac{k\left(M_a + M_s + M_p + M_q\right) + e\left(N_a + N_s + N_p + N_q\right)}{W_{eff}} = 0 \tag{4}$$

f_y	elastic limit of structural steel (or wrought iron)
N_a	axial compression due to the self weight of the steel
N_s	axial compression due to the sand fill
N_p	axial compression due to the asphalt layer
N_q	axial compression due to the traffic actions
M_a, M_s, M_p, M_q	moments due to the different aforementioned actions
A_{eff}	effective area of the cross-section when subject to uniform compression
W_{eff}	effective section modulus of the cross-section when subject only to moment about the relevant axis
χ	reduction factor for the relevant buckling mode
e	shift of the relevant centroidal axis when the cross-section is subject to uniform compression
k	factor which takes into account the distribution of the moments and the characteristics of the cross-section

The parameters of the variables involved in the LSF that are assumed to lie behind the rules of the codes are taken from the literature [5]. This LSF and the parameters of the variables (mean value, standard deviation, probability distribution) may now be introduced in a computer program [8] which handles the variables in accordance with the method from [6] and calculates the FOSM reliability index β_{code}. In the present case we obtain β_{code} = 4.06.

The third step of the verification consists of the calculation of the reliability index, β, of the actual member. *A priori* values for the parameters of the variables (Table 1), are either taken directly or interpreted from [2, 5, 9, 10] and introduced in the LSF (4). The FOSM reliability index is calculated to be β = 1.12.

Obviously, according to the inequality (3), the member under consideration is not safe. Site data should therefore be collected in order to improve the load and resistance models for the continuation of the evaluation (Figure 2).

Variable	Type	bias μ_X/X_{nom}	cov σ_X/μ_X	Nominal value X_{nom}	Mean μ_X	Standard deviation σ_X	Influence coefficient α_X^*	Design value X^*
f_y	LN	1.195	0.115	220 N/mm^2	263	30.3	0.826	234.8
N_a	N	1.01	0.03	234 kN	236.3	7.1	-0.025	236.5
N_s	N	1.20	0.25	273 kN	327.6	81.9	-0.29	354.3
N_p	N	1.20	0.25	82 kN	98.4	24.6	-0.087	100.8
N_q	Gumbel	0.88	0.125	1070 kN	941.6	117.7	-0.45	980.9
M_a	N	1.01	0.03	5.9 kNm	6.0	0.18	-0.004	6.0
M_s	N	1.20	0.25	9.5 kNm	11.4	2.85	-0.061	11.6
M_p	N	1.20	0.25	2.8 kNm	3.4	0.85	-0.018	3.42
M_q	Gumbel	0.88	0.125	43 kNm	37.8	4.7	-0.094	37.48
A_{eff}	N	1.02	0.01	14061.6 mm^2	14342	143.4	0.034	14340
W_{eff}	N	1.02	0.01	$1.68 \cdot 10^6$ mm^3	$1.71 \cdot 10^6$	$1.71 \cdot 10^4$	0.038	$1.71 \cdot 10^6$
χ	N	1.05	0.024	1.0	1.05	0.025	0.081	1.048
e	N	1.02	0.01	82.5 mm	84.2	0.84	-0.025	84.22
k	N	1.04	0.02	1.15	1.20	0.024	-0.025	1.2

***Table 1** Assumed values of the parameters of the variables for the estimation of β and results of FOSM analysis*

4.2.3 Conclusion

In addition to the reliability index, β, the method according to [6] provides the design values, X*, and the importance factors, α_X^*, corresponding to the variables involved in the LSF (Table 1). The design values, X*, correspond to the most probable set of values of the variables at failure. The importance factor is a function of the relative importance of a given basic variable within a given LSF. The greater the absolute value of α_X^* (the importance factor is negative for variables which have an unfavourable effect on safety), the bigger the influence of the variation of the corresponding variable on the reliability index. In the above example the yield strength of wrought iron, f_y, and axial compression due to traffic actions, N_q, are most critical. For these variables, updating efforts would be most effective.

4.3 Collection of site data - Planning and execution

4.3.1 Overview

The definition of a test program includes the choice of the parameters which should be updated, the definition of the method of observation and recording, the selection of test specimens, test conditions and arrangements, the number of tests and the method of evaluation. The execution of tests should be in accordance with the planning, and the measurement techniques in accordance with the required tolerances. For the evaluation of the test results, methods should be used which enable an easy introduction of the updated information in the calculation models. In the present case, according to 4.2.3 updating is carried out for the wrought iron yield strength and the traffic actions. For two reasons it is also decided to carry out measurements of the actual dimensions of wrought iron member cross-sections: the influence of corrosion is to be assessed and the assumed dimensional variation in the reliability analysis (4.2.2) corresponds to modern welded steel elements, for which fabrication tolerances are very small, and not to wrought iron members.

In the following, some information about the planning and execution of site data collection is given. Section 4.4 contains some thoughts on test evaluation, and the obtained site specific data is summarised in Table 2.

4.3.2 Material properties

Material properties are determined from miniaturised specimens, which can be drilled from structural members without reducing their resistance [11]. In the present case for example, the

dimensions of the cylindrical specimens for tensile tests are: 40 mm of total length and 3 mm of diameter. Chosen test temperatures are room temperature (20°C) and -20°C corresponding to the lowest service temperature expected to occur within the intended remaining life of the structure.

Test samples should be representative and a sufficient number should be taken in order to determine variability with adequate certainty. In normal daily practice, however, only a limited number of tests can be carried out for economical reasons. In the present case for example, the number of tensile tests is eight. In section 4.4, the influence of the number of tests on the characteristic value of the wrought iron yield strength is discussed.

4.3.3 Cross-section area

The influence of the severe corrosion of the truss girder bottom U-section members is directly taken into account in the corresponding resistance model by introducing an equivalent cross-section (Figure 3). The influence of the dimensional variation due to corrosion and fabrication tolerances on the structural resistance of the other members is to be assessed. This is done by extensive measurement of the actual dimensions of wrought iron cross-sections.

4.3.4 Traffic actions

For economical reasons, neither vehicle surveys nor measurements of the effects of vehicle actions on the bridge with a view to obtaining data describing traffic actions are possible in the present case. Only traffic counting can be carried out: a daily traffic volume of 10059 vehicles, of which 12.5% are Heavy Goods Vehicles, is physically measured. This means that an average of 1257 HGV per day cross this urban bridge. Furthermore, frequent traffic jams are observed due to the traffic lights situated at both ends of the bridge. It is also known that the percentage of overloaded HGV in Spain is around 25% [12]. The effects of traffic actions on road bridges is described by a certain frequency distribution which determines the extreme action effects to be considered during the assessment of structural safety [5]. These effects may be obtained based on numerical simulations by generating random traffic actions for the considered traffic type [5, 9].

4.4 Evaluation of tests

If only a limited number of tests on material samples are available, as normal in daily practice, the evaluation of test results according to standard statistical methods may lead to unrealistic low characteristic or design values [13]. This drawback can be avoided, if the evaluation of test samples with a limited number of tests is carried out according to statistical models which permit the introduction of prior knowledge. Based on knowledge about the distribution of the investigated variable, a posterior distribution is derived in combination with the obtained test results. Such an approach is applied in the present study. In the case of the wrought iron strength, for example, a mean value of the yield strength m_{fy} = 225 N/mm^2 and a standard deviation of s_{fy} = 17.1 N/mm^2 are obtained from the sample of eight tensile tests. The corresponding characteristic value, which is based on a 5% fractile with a confidence level of 75%, evaluated with standard statistical methods [13], is f_{yk} = 187.5 N/mm^2. It is known from previous experience that for the yield strength of wrought iron a lognormal distribution can be expected. Furthermore, the sample standard deviation, s_{fy}, underestimates the standard deviation of the whole population, σ_{fy}, depending on the sample size. Taking into account this prior information, the estimate for the characteristic value of the yield strength is f_{yk} = 196.8 N/mm^2.

5. Introduction of test results in the calculation models

5.1 Overview

As mentioned in chapter 3, a full reliability analysis is not considered viable for the investigated bridge. A simplified deterministic method should therefore be used. The aim of a deterministic assessment of structural safety is to verify that the inequality (2) is satisfied by using nominal values of basic variables and partial safety factors in order to obtain the values that they would have at the design point in a reliability analysis [5]. The link between reliability concepts and deterministic methods is the design point which is the most probable failure point on a limit state

surface [5]. The relation between the design point, partial safety factor and nominal value is given by

$$X^* = \gamma_X \cdot X_{nom} \tag{5}$$

X^* value of the basic variable at the design point
γ_X partial safety factor
X_{nom} nominal value of the basic variable

The Limit State Function is the same for both methods (reliability and deterministic), only the representation of the variables is different. Partial safety factors, which are introduced in a deterministic analysis, are therefore attributed individually to the variables in the LSF and vary according to the degree of uncertainty and the importance of the variable within the LSF. The aim of the collection of site specific data is the reduction of the uncertainty associated with the variables. The influence of this change can not be considered explicitly in a deterministic assessment (only changes in the mean value of a variable can be accounted for). As mentioned in chapter 3, the site specific data is therefore used to calibrate updated deterministic models of action effects and resistance, by applying reliability methods to the simplified structural model according to 4.2.1.

5.2 Calibration procedure

According to the *axiom* mentioned in 4.2.2, the calibration procedure consists of the following five steps:

- Dimensioning of the existing structure according to a consistent set of codes,
- Calculation of the reliability index, β_{code}, for this structure,
- Calculation of the reliability index, β_{upd}, for the actual structure using the updated parameters of the variables. β_{upd} may be greater or smaller than β_{code}, depending mainly on the state of the structure (corrosion) and the aggressivity of the actual traffic.
- Find the required actual resistance, $R_{upd.req}$, by multiplying the actual resistance, R_{upd}, by a factor, κ_R, in a way that results $\beta_{upd} = \beta_{code}$ for the actual effect of actions, S_{upd} (Figure 5).
- Derive partial safety factors, in analogy with equation (5), which can be applied to the nominal values of basic variables (S_{nom} for action effects and R_{nom} for resistance) in a deterministic assessment:

$$\gamma_{S,upd} = \frac{S^*_{upd}}{S_{nom}} \tag{6}$$

$\gamma_{S,upd}$ updated partial safety factor for action effects
S^*_{upd} updated action effect at the design point
S_{nom} nominal value of the action effect

$$\gamma_{R,upd} = \frac{\kappa_R \cdot R_{nom}}{R^*_{upd.req}} \tag{7}$$

$\gamma_{R,upd}$ updated partial safety factor for resistance
$R^*_{upd.req}$ updated required resistance at the design point
R_{nom} nominal value of the resistance
κ_R factor for the calculation of the required actual resistance

The updated partial safety factors, which take into account the influence of a change in uncertainty associated with the variables and are attributed individually to the basic variables in a LSF, can now be used in a deterministic assessment (using a more refined structural model) of structural safety, together with the nominal values of action effects and resistance. The requirement for structural safety can therefore be derived from the inequality (2) and is expressed by the following condition:

$$\gamma_{S,upd} \cdot S_{nom} \leq \frac{R_{nom}}{\gamma_{R,upd}} \tag{8}$$

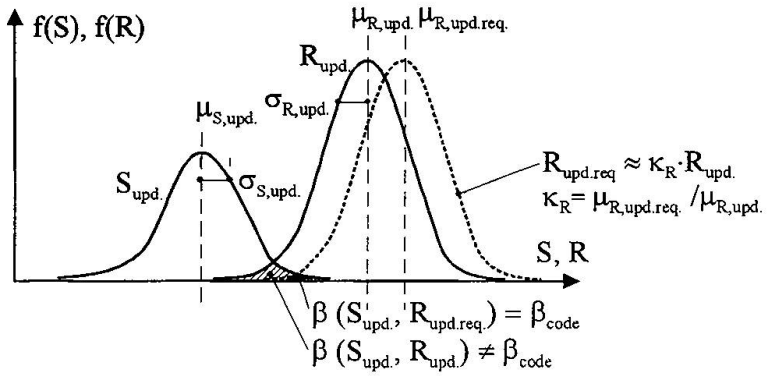

Fig. 5 Calibration of updated load and resistance models

5.3 Case study

The first two steps of the calibration procedure correspond to the first two steps of the reliability analysis from 4.2.2. Therefore, the reliability index according to the current codes is: $\beta_{code} = 4.06$. The collection and evaluation of site data according to 4.3 and 4.4 results in updated parameters of the corresponding variables, listed in Table 2.

Variable	Type	bias $\frac{\mu_{X,upd}}{X_{nom}}$	cov $\frac{\sigma_{X,upd}}{\mu_{X,upd}}$	Mean $\mu_{X,upd}$	Standard deviation $\sigma_{X,upd}$
f_y	LN	1.023	0.079	225 N/mm^2	17.7
N_q	Gumbel	0.80	0.125	856 kN	107
M_q	Gumbel	0.80	0.125	34.4 kNm	4.3
A_{eff}	LN	1.013	0.023	14249.4 mm^2	336.6
W_{eff}	LN	1.013	0.023	$1.7 \cdot 10^6$ mm^3	$3.9 \cdot 10^4$

Table 2 Updated parameters of the variables

Action effects				Resist.
Iron $\gamma_{Ga,upd}$	Sand $\gamma_{Gs,upd}$	Asph. $\gamma_{Gp,upd}$	Traff. $\gamma_{Q,upd}$	$\gamma_{R,upd}$
1.01	1.45	1.3	1.4	1.06

Table 3 Updated partial safety factors

For the other variables of the LSF (4), the parameters from Table 1 are adopted. The calculation of the FOSM reliability index for the actual structure gives $\beta_{upd} = 0.493$. This value is even lower than the one calculated in 4.2.2 using default probabilistic models of action effects and resistance. This is mainly due to the fact that in the bridge under investigation the elastic limit of the wrought iron is lower than usual values for this type of material. For the aforementioned factor, κ_R, a value of $\kappa_R = 1.484$ is found. The values of the basic variables of the LSF (4) at the design point, $X^*_{upd.(req)}$, result from the FOSM analysis, carried out for S_{upd} and $R_{upd.req.}$ These values are then used to derive updated partial safety factors according to the equations (6) and (7). The obtained results are listed in Table 3. In a detailed deterministic assessment with updated models of action effects and resistance (according to (8)) it is now possible to determine the structural elements, nodes and riveted connections which need to be strengthened (Figure 2). The proposed solution for the strengthening is presented in [12].

6. Conclusions

A proper assessment of an existing bridge based on incomplete or defective information may be completely wrong. Therefore, correct updating of data is probably the most important step in a bridge evaluation. For the choice of the test and inspection programme some guidelines should be observed:

- The expected structural behaviour, loading and environmental conditions should be investigated by a qualitative analysis.

- Based on the results of the preliminary analysis, the objectives of the tests can be formulated and correct choices for the test programme are possible.
- The tests should be undertaken following the established plan.
- The evaluation of test samples with a limited number of tests should be carried out taking into account prior knowledge in order to avoid unrealistic low design values.

There is a need for simplified load and resistance models for the assessment of existing bridges. Furthermore, methods should be developed which enable an easy introduction of the collected site data in these simplified models.

Acknowledgements

Some of the presented work has been carried out as a part of the refurbishment project for the Zamora bridge, commissioned by the "Dirección General de Carreteras" of the Ministry of Public Works. The department of Material Sciences of the University of Madrid (Prof. M. Elices Calafat, Prof. A. Valiente Cancho) is also thanked for the carefully conducted material testing.

References

1. RPM-95. Recommendations for the design of steel bridges. Ministry of public works, Madrid, 1996. (in Spanish)
2. KUNZ, P. Probabilistic method for the evaluation of fatigue safety of existing steel bridges. Lausanne, Swiss Federal Institute of Technology, 1992. (thesis n° 1023, in German)
3. TANNER, P. und HIRT, M.A. Überlegungen zur Restlebensdauer schweisseiserner Brücken am Beispiel der Basler Wettsteinbrücke. Stahlbau, Vol. 60, 1991, p 211-219.
4. Draft IAP-96. Actions on road bridges. Ministry of public works, Madrid, 1996. (in Spanish)
5. BAILEY, S.F. Basic principles and load models for the structural safety evaluation of existing road bridges. Lausanne, Swiss Federal Institute of Technology, 1996. (thesis n° 1467)
6. HASOFER, A.M. and LIND, N.C. Exact and Invariant second moment code format. Journal of the Engineering Mechanics Division ASCE, Vol. 100, 1974, p 111-121.
7. SCHNEIDER, J. Some thoughts on the reliability assessment of existing structures. Structural Engineering International, Zürich, Volume 2, N° 1, 1992, p 13-18.
8. VaP. Computer Program VaP (Variables Processor) 1.5 for Windows. Zürich, IBK-Swiss Federal Institute of Technology, 1996.
9. SOBRINO, J.A. et al. Structural evaluation of existing concrete bridges. Assessment and strengthening of a prestressed concrete box-girder bridge. In: Bridge Assessment, Management and Design (Barr, Evans, Harding, Eds.), Amsterdam, Elsevier Publishing Company, 1994. ISBN 0-444-82063-9.
10. VARONA, J.M., GUTIERREZ, S.F. y GONZALEZ, J.J. Comportamiento en fatiga de puentes metálicos antiguos de ferrocarril. Revista de Obras Públicas, Vol. 139, N° 3312, 1992, p 79-87.
11. HENSEN, W. Grundlagen für die Beurteilung der Weiterverwendung alter Stahlbrücken. RWTH Aachen, 1992. (D82 Diss. TH Aachen)
12. TANNER, P. et al. Strength and functionality - A case study. In: Bridge Assessment, Management and Design (Barr, Evans, Harding, Eds.), Amsterdam, Elsevier Publishing Company, 1994. ISBN 0-444-82063-9.
13. VAN STRAALEN, I., VROUWENVELDER, T. Comparison of statistical evaluation models. Proceedings, IABSE - Colloquium "Basis of Design and Actions on Structures. Background and application of Eurocode 1", Delft, March 27-29, 1996.